**Repository of the Max Delbrück Center for Molecular Medicine (MDC)
in the Helmholtz Association**

https://edoc.mdc-berlin.de/18974

# NF-κB signaling in tanycytes mediates inflammation-induced anorexia.

Böttcher M., Müller-Fielitz H., Sundaram S.M., Gallet S., Neve V., Shionoya K., Zager A., Quan N., Liu X., Schmidt-Ullrich R., Haenold R., Wenzel J., Blomqvist A., Engblom D., Prevot V., Schwaninger M.

# Journal Pre-proof

NF-κB signaling in tanycytes mediates inflammation-induced anorexia

Mareike Böttcher, Helge Müller-Fielitz, Sivaraj M. Sundaram, Sarah Gallet, Vanessa Neve, Kiseko Shionoya, Adriano Zager, Ning Quan, Xiaoyu Liu, Ruth Schmidt-Ullrich, Ronny Haenold, Jan Wenzel, Anders Blomqvist, David Engblom, Vincent Prevot, Markus Schwaninger

Please cite this article as: Böttcher M, Müller-Fielitz H, Sundaram SM, Gallet S, Neve V, Shionoya K, Zager A, Quan N, Liu X, Schmidt-Ullrich R, Haenold R, Wenzel J, Blomqvist A, Engblom D, Prevot V, Schwaninger M, NF-κB signaling in tanycytes mediates inflammation-induced anorexia, *Molecular Metabolism*, https://doi.org/10.1016/j.molmet.2020.101022.

This is a PDF file of an article that has undergone enhancements after acceptance, such as the addition of a cover page and metadata, and formatting for readability, but it is not yet the definitive version of record. This version will undergo additional copyediting, typesetting and review before it is published in its final form, but we are providing this version to give early visibility of the article. Please note that, during the production process, errors may be discovered which could affect the content, and all legal disclaimers that apply to the journal pertain.

# NF-κB signaling in tanycytes mediates inflammation-induced anorexia

Mareike Böttcher[1,#], Helge Müller-Fielitz[1,9,#], Sivaraj M. Sundaram[1], Sarah Gallet[2,3], Vanessa Neve[1], Kiseko Shionoya[4], Adriano Zager[4], Ning Quan[5], Xiaoyu Liu[5], Ruth Schmidt-Ullrich[6], Ronny Haenold[7,8], Jan Wenzel[1,9], Anders Blomqvist[4], David Engblom[4], Vincent Prevot[2,3], Markus Schwaninger[1,9]

[1]Institute for Experimental and Clinical Pharmacology and Toxicology, University of Lübeck, 23562 Lübeck, Germany;
[2]Inserm, Laboratory of Development and Plasticity of the Neuroendocrine Brain, Jean-Pierre Aubert Research Centre, U1172 Lille, France;
[3]University of Lille, FHU 1000 days for Health, School of Medicine, U1172 Lille, France;
[4]Department of Clinical and Experimental Medicine, Linköping University, S-581 85 Linköping, Sweden;
[5]Charles E. Schmidt College of Medicine and Brain Institute, Florida Atlantic University, Jupiter, FL 33458, USA;
[6]Department of Signal Transduction in Tumor Cells, Max-Delbrück-Center (MDC) for Molecular Medicine, 13125 Berlin, Germany;
[7]Leibniz Institute on Aging - Fritz Lipmann Institute (FLI), 07745 Jena, Germany;
[8]Matthias Schleiden Institute of Genetics, Bioinformatics and Molecular Botany, Friedrich Schiller University Jena, 07743 Jena, Germany.
[9]DZHK (German Centre for Cardiovascular Research), partner site Hamburg/Kiel/Lübeck, Lübeck, Germany.
# shared first authorship




Corresponding author: Markus Schwaninger, University of Lübeck, Institute for Experimental and Clinical Pharmacology and Toxicology, Ratzeburger Allee 160, 23562 Lübeck, Germany, Tel.: +49-451-3101-7200, E-Mail: markus.schwaninger@uni-luebeck.de

# Abstract

***Objectives***: Infections, cancer and systemic inflammation elicit anorexia. Despite the medical significance of this phenomenon, the question of how peripheral inflammatory mediators affect the central regulation of food intake is incompletely understood. Therefore, we have investigated the sickness behavior induced by the prototypical inflammatory mediator IL-1β.

***Methods***: IL-1β was injected intravenously. To interfere with IL-1β signaling we deleted the essential modulator of NF-κB signaling (*Nemo*) in astrocytes and tanycytes.

***Results***: Systemic IL-1β increased the activity of the transcription factor NF-κB in tanycytes of the mediobasal hypothalamus (MBH). By activating NF-κB signaling, IL-1β induced the expression of cyclooxygenase-2 (Cox-2) and stimulated the release of the anorexigenic prostaglandin $E_2$ ($PGE_2$) from tanycytes. When we deleted *Nemo* in astrocytes and tanycytes, the IL-1β-induced anorexia was alleviated whereas the fever and lethargy response were unchanged. Similar results were obtained after selective deletion of *Nemo* exclusively in tanycytes.

***Conclusions***: Tanycytes form the brain barrier that mediates the anorexic effect of systemic inflammation in the hypothalamus.

**Key words**

Tanycytes, inflammation-induced anorexia, IL-1β, NEMO

## 1. Introduction

Cachexia and anorexia in chronic diseases, like HIV infection or cancer, worsen the outcome and increase mortality [1-3]. A prominent mechanism underlying cachexia is thought to be systemic inflammation [4]. Inflammation induces the so-called sickness response including fever, lethargy, and anorexia. This repertoire of physiological reactions is conserved during evolution, and, in another context, seems to have a physiological benefit. Apparently, it helps mobilize the resources required to combat specific causal pathogens [5]. Infection-induced anorexia increases the host tolerance to bacterial inflammation [6]. In turn, pathogens have developed means to manipulate the host response. *Salmonella typhimurium* modulates host survival and promotes disease transmission to other subjects by interfering with the maturation of IL-1β that induces anorexia [7].

Pro-inflammatory cytokines such as IL-1β are essential for the host response to inflammation and infection. In accordance with this notion, IL-1β is induced by local or systemic inflammation and, when administered systemically, triggers many of the characteristic physiological changes, including anorexia, fever and lethargy [8]. Upon binding to its membrane receptor IL-1R1 that is widely expressed in the CNS [9], IL-1β stimulates a pro-inflammatory signaling cascade that is mediated by the adaptor protein Myd88. In line with this, global deletion of Myd88 prevented inflammation-induced anorexia [10; 11]. Downstream of Myd88, IL-1β activates the canonical NF-κB signaling pathway that involves the protein kinase IKK complex. The latter consists of two enzymatic subunits and the essential regulatory subunit NEMO. Among the hundreds of NF-κB target genes, *Ptgs2* (*Cox-2*) stands out in the context of inflammation-induced anorexia because blocking its activity by common analgesic and antipyretic drugs, such as acetylsalicylic acid or celecoxib, reduces fever and inflammation-induced anorexia [12; 13]. Thus, a precise picture of the molecular signaling pathways that mediate inflammation-induced anorexia emerges, but less is known about which cellular and anatomic routes convey the inflammatory signal to the hypothalamic centers that regulate food intake. With a molecular weight of about 17 kD, IL-1β is too big for

1 unassisted diffusion through brain barriers, although there are some reports that small

2 amounts of radioactively labeled IL-1β can enter the brain [14]. Endothelial cells of the

3 blood-brain barrier are a key hub for transmitting fever inducing signals into the

4 hypothalamus [15-18]. In marked contrast, endothelial cells do not mediate anorexia that is

5 induced by peripheral inflammation [17; 19; 20].

6 In the MHB, tanycytes represent another barrier forming cell type [21]. These specialized

7 glial cells separate the vascular compartment and circumventricular organs from brain

8 parenchyma and cerebrospinal fluid (CSF). They line the wall and floor of the 3rd ventricle in

9 the MHB and project into the ventromedial nucleus (VMH) and arcuate nucleus (ARC), the

10 hypothalamic centers that regulate appetite [21]. A link to metabolic regulation is further

11 suggested by the observation that tanycytes are able to sense glucose [22] and ghrelin [23]

12 and to transport leptin into the CNS [24]. However, their physiological function in regulating

13 food intake still remains largely elusive.

14 In this study we have investigated the cellular pathways mediating IL-1β-induced anorexia.

15 Systemic IL-1β administration stimulated NF-κB activity in tanycytes of the MHB. To inhibit

16 NF-κB signaling we deleted the essential IKK subunit NEMO in glial cells and tanycytes

17 demonstrating that IL-1β-induced anorexia at least partially depends on tanycytic NF-κB

18 signaling. These data suggest tanycytes as an important route to transfer peripheral immune

19 signals into the CNS and modulate the energy supply under inflammatory conditions.

# 2. Materials and methods

## 2.1. Animals

Animal experiments were approved by the local ethic committee (Ministerium für Energiewende, Landwirtschaft, Umwelt, Natur und Digitalisierung in Kiel, Germany; Animal Care and Use Committee at Linköping University, Sweden) and were in accordance with the EU Directive 2010/63/EU for animal experiments. For all experiments we used male 8-12-weeks old mice that were on a C57Bl/6 background. They were housed on a light-dark cycle of 12 h and at a temperature of 22°C, except for body temperature measurements, which were performed under near thermo-neutral conditions (29°C). All mice had *ad-libitum* access to a standard laboratory diet (2.98 kcal/g; Altromin, Hannover, Germany; 2.91 kcal/g, Lantmännen, Malmö, Sweden) and water, unless indicated otherwise. To investigate the influence of NF-κB in tanycytes under pro-inflammatory conditions, *Nemo*<sup>FL</sup> mice [25] were crossed with mice which express a tamoxifen-inducible Cre recombinase under the glia-specific *Glast* promoter (*GlastCreER*<sup>T2</sup>) [26]. At an age of 8-10 weeks, tamoxifen was injected (1 mg, every 12 h over 5 days) to induce *Nemo* knockout in glial cells (*Nemo*<sup>gliaKO</sup>). Tamoxifen-treated Cre-negative littermates were used as controls (*Nemo*<sup>FL</sup>). NF-κB reporter mice (κ-EGFP) [27] and *Il1r1*<sup>GR/GR</sup> reporter mice [28] have been described previously. To specifically delete *Nemo* in tanycytes a rAAV approach was used that we have recently developed [29]. We tested the cell specificity of AAV-Dio2-iCre-2A-EGFP and *GlastCreER*<sup>T2</sup> with the Cre reporter mouse line Ai14 [30]. All mice were randomly allocated to treatment groups. Investigators were blinded for treatment or genotype of mice or both whenever possible. Mice were only excluded from analysis if they did not survive during surgical procedures or if samples could not be obtained.

## 2.2. Primary tanycyte cell culture

Tanycytes were isolated from P10 Sprague Dawley rats (Janvier) by dissecting the wall of the 3<sup>rd</sup> ventricle of the MBH as described previously [31]. A tanycyte cell culture contained tissue from 20 pups, which had been collected in culture medium (DMEM high-glucose

1  medium containing 10% fetal calf serum, 1% penicillin/streptomycin, and 2 mM L-glutamine,

2  Thermo Fisher) on ice. To separate tanycytes, samples were scraped through a nylon mesh

3  (20 μm, Merck Millipore), centrifuged and cells were resuspended in fresh culture medium.

4  No medium change was done within the first 10 days, afterwards medium was changed twice

5  a week. Cultures that reached confluency were split by trypsin/ETDA digestion and plated in

6  6-well plates for further experiments. After 3 weeks the medium of the cultures was changed

7  to starvation medium (DMEM/F12 without phenol red, 1% penicillin/streptomycin and 2 mM

8  L-glutamine, all from Thermo Fisher). One h before the experiment started, cells were

9  changed to experimental medium (DMEM/F12 without phenol red, 1%

10  penicillin/streptomycin, 2 mM L-glutamine (all from Thermo Fisher) and 0.15% insulin and

11  0.3% putrescine (last two from Sigma-Aldrich, USA)) and treated with rat recombinant IL-1β

12  (0.25 μg/ml, Peprotech) or PBS. Cells were harvested after 0, 2, 4, 8 and 24 h by washing

13  them 3 times with ice-cold PBS and shock freeze on dry ice. The purity of the primary cell

14  culture was confirmed by immunostaining of vimentin, GFAP, and CD11b as well as by qRT-

15  PCR.

16  To inhibit NF-κB, tanycytes were treated prior to the experiment with 25 μM BMS-345541

17  (dissolved in DMSO, Axon Medchem BV) or 0.25% DMSO. After 30 min cells were treated

18  with rat recombinant IL-1β (0.25 μg/ml, Peprotech). The supernatant was collected after 2

19  and 8 h of treatment and the cells were harvested. Secreted prostaglandin E2 was measured

20  by using the Prostaglandin E2 Elisa kit (Cayman) according to the manufacturer's

21  instructions.

22  **2.3. AAV production and stereotaxic vector injections**

23  AAV with a mosaic capsid of serotype 1 and 2 (1:1) were generated as described and

24  purified by AVB Sepharose affinity chromatography [29]. For each vector, the genomic titer

25  was determined by quantitative PCR (qPCR) using primers against WPRE (WPRE forward

26  primer: 5′-TGC CCG CTG CTG GAC-3′; WPRE reverse primer: 5′-CCG ACA ACA CCA

27  CGG AAT TG-3′) as described previously [29]. For stereotaxic injections, *Nemo*[FL] mice were

1  anesthetized with ketamine (65 µg/g, Ketavet™, Pfizer) and xylazine (14 µg/g, Rompun™,

2  Bayer) before they were fixed in the stereotaxic frame (David Kopf Instruments). During the

3  procedure the body temperature was maintained at 37°C by a heating plate. After drilling a

4  small borehole between bregma and lambda, AAV vectors ($10^{11}$ genomic particles in 2 µl)

5  were injected into the lateral ventricle (anteroposterior –0.1 mm, mediolateral –0.9 mm,

6  dorsoventral from the skull surface –2.3 mm relative to bregma) as described previously [29].

7  Injections were performed over 5 min and the cannula stayed in place for another 10 min to

8  avoid backflow of the vectors. The scalp was sutured and the animals were treated with

9  carprofen (5 mg/kg; s.c.) for 2 days. *Nemo*[FL] mice received either AAV-Dio2-Cre-2A-EGFP to

10  express the Cre recombinase under the tanycytic specific *Dio2* promoter (*Nemo*[tanKO]) or the

11  control vector AAV-Dio2-EGFP without Cre activity (*Nemo*[Con]).

12  **2.4. IL-1β effects on feeding and related parameters**

13  Mice received PBS and, after a lag time of 2 days, recombinant mouse IL-1β (20 µg/kg, i.v.,

14  Peprotech). Both treatments were administered by injection into the tail vein under

15  anesthesia (4% isoflurane) one h before lights turned off. At the same time, the food was

16  removed and returned at beginning of the dark phase. Food and water intake as well as body

17  weight, respiratory exchange ratio (RER) and energy expenditure (EE) were monitored over

18  24 h by indirect calorimetry.

19  **2.5. Measurement of cytokine concentrations in plasma**

20  For measuring cytokine concentrations in plasma, *Nemo*[FL] and *Nemo*[gliaKO] mice were treated

21  with IL-1β (20 µg/kg, i.v., Peprotech) and were sacrificed after 4, 8 and 24 h by a lethal dose

22  of pentobarbital (150 µg/g, i.p.). Blood samples were obtained by heart puncture in EDTA

23  vials (Sarstedt). IL-1β, IL-6, and TNF were measured in plasma by MILLIPLEX mouse kit

24  (Merck Millipore) according to the manufacturer's instructions.

25  **2.6. Reporter mice for monitoring NF-κB activation and *Il1r1* expression**

26  κ-EGFP mice were used to identify cells with NF-κB activity in the MBH after IL-1β treatment.

27  Therefore, κ-EGFP mice were treated either with mouse recombinant IL-1β (20 µg/kg, i.v.) or

1    with PBS under 4% isoflurane anesthesia. Eight h later mice were sacrificed by a lethal dose

2    of pentobarbital (150 µg/g, i.p.). Brains were post-fixed in paraformaldehyde (PFA, 4%),

3    cryoprotected by incubation in sucrose (30% in PBS) for 24 h and stored at -80°C. We

4    counted EGFP-positive cell bodies.

5    To localize *Il1r1* expression we used *Il1r1*[GR/GR] mice [28]. To enhance IL-1R1 expression, the

6    animals were treated with LPS (120 µg/kg, E. coli serotype 0111:B4, i.p.) and perfused after

7    6 h with 0.9% saline at room temperature, followed by ice-cold PFA (4%, pH 9.5). Brains

8    were post-fixed for 2 h and cryoprotected for 48 h.

9    **2.7. Telemetric monitoring of mice**

10    Two weeks after inducing recombination with tamoxifen, mice were anesthetized with

11    isoflurane and transmitters (TA-F10, Data Science International) were intraperitoneally

12    implanted. For postoperative pain management we administered carprofen (5 mg/kg, s.c.)

13    every 12 h for 2 days. Seven days after implanting transmitters, mice were treated with IL-1β

14    (20 µg/kg, i.v.) 3 h after lights-on and the body temperature and activity were monitored.

15    Novelty stress was evaluated during animal care. After *Nemo*[FL] and *Nemo*[gliaKO] mice carrying

16    telemetric transmitters were transferred to new cages during the inactive light phase, body

17    temperature and activity were recorded.

18    **2.8. Indirect calorimetry**

19    For indirect calorimetry 3 weeks after tamoxifen (*Nemo*[FL] and *Nemo*[gliaKO]) or virus injection

20    (*Nemo*[con] and *Nemo*[tanKO]), mice were kept in ventilated cages of the PhenoMaster System

21    (TSE, Germany) for 7 days on a 12 h light/dark cycle at 23°C. After 3 days of adaption PBS

22    and two days later IL-1β (20 µg/kg, i.v.) were intravenously injected 1 h before lights turned

23    off according to the same protocol as described above. Food and water intake were

24    automatically monitored every 30 min. $O_2$ and $CO_2$ concentrations in the cages were

25    measured every 30 min to determine EE and RER. All measurements ran simultaneously.

1   EE was calculated as 3.941 x $O_{2\ consumed}$ [l] + 1.106 x $CO_{2\ produced}$ [l]. The measurements after

2   PBS treatment served as intra-individual controls for the IL-1β treatment.

## 2.9. Isolation of tanycytes and RT-PCR

4   For laser microdissection, native coronal cryosections (25-µm thick) of the MBH were

5   mounted on membrane slides 1.0 PEN (Zeiss, Germany). Tanycytes were microdissected

6   using the Axiovert 200 M microscope (Zeiss, Germany) and a system with a pulsed 337-nm

7   UV laser (PALM MicroBeam, PALM Microlaser Technologies) and the laser-pressure

8   catapulting mode. Areas corresponding to α-tanycytes (about 10,000 µm²) and to the ARC

9   (about 60,000 µm²) were dissected on 8 sections of the MBH (bregma −1.58 mm to −1.7

10   mm) and pooled. RNA was isolated using the Absolutely RNA Nanoprep Kit (Agilent

11   Technologies) according to the manufacturer's instructions. RNA was transcribed into cDNA

12   by the reverse transcriptase AMV (Avian Myeloblastosis Virus; Cloned AMV First-Strand

13   cDNA Synthesis Kit, Invitrogen) with oligo(dT) primers and diluted 1:1 in diethyl

14   pyrocarbonate (DEPC) water (Sigma Aldrich). For real-time PCR the following primers were

15   used: *Ptgs2* forward primer 5′- CTG ACC CCC AAG GCT CAA AT -3′, *Ptgs2* reverse primer

16   5′- AAG TCC ACT CCA TGG CCC AG -3′, PCR product 124 bp; *Agrp* forward primer 5′-

17   CGC TTC TTC AAT GCC TTT TGC-3′, *Agrp* reverse primer 5′-ATT CTC ATC CCC TGC

18   CTT TGC-3′, PCR product 108 bp; *Npy* forward primer 5′-TCG CTC TAT CTC TGC TCG

19   TGT G-3′, *Npy* reverse primer 5′-AGT ATC TGG CCA TGT CCT CTG C-3′, PCR product

20   105 bp; *Pomc* forward primer 5′-AGC GTT ACG TGG CTC ATG A-3′; *Pomc* reverse

21   primer 5′-TGG AAT GAG AAG ACC CCT GCA-3′, PCR product 125 bp; and *Gapdh* forward

22   primer 5′-CCT ACC CCC AAT GTA TCC GTT-3′, *Gapdh* reverse primer 5′-TAG CCC AGG

23   ATG CCC TTT AGT-3′, PCR product 122 bp. Real-time PCR was performed with the

24   Platinium SYBR Green qPCR Super Mix (Invitrogen) according to the following protocol: 2

25   min at 50 °C, 2 min at 95 °C, 15 s at 95 °C, and 1 min at 60 °C (40 cycles). Quantified results

26   were normalized to *Gapdh* using the ΔΔCt method.

1  From primary rat tanycytes RNA was extracted with the help of NucleoSpin columns

2  (Macherey-Nagel). For quantification of gene expression the following primers were used:

3  *Ptgs2* forward primer  5′-CTC AGC CAT GCA GCA AAT CC-3′, *Ptgs2* reverse primer 5′-

4  GGG TGG GCT TCA GCA GTA AT-3′, PCR product 172 bp; *Il1b* forward primer 5′-GGC

5  TTC CTT GTG CAA GTG TC-3′, *Il1b* reverse primer 5′-CCC AAG TCA GGG CT TGG AA-

6  3′, PCR product 152 bp; *Il1r1* forward primer 5′-TGT GGC TGA AGA GCA CAG AG-3′, *Il1r1*

7  reverse primer 5′-TGG ATC CTG GGT CAG CTT C-3′, PCR product 172 bp; *Vcam1* forward

8  primer 5′-GGA AAT GCC ACC CTC ACC TT-3′, *Vcam1* reverse primer 5′-AAC AGT AAA

9  TGG TTT CTC TTG AAC A-3′, PCR product 132 bp; and *Gapdh* forward primer 5′-CCT ACC

10 CCC AAT GTA TCC GTT-3′, *Gapdh* reverse primer 5′-TAG CCC AGG ATG CCC TTT AGT-

11 3′, PCR product 122 bp.

12 For FACS-sorting of tanycytes we used a protocol reported previously [32]. Briefly, tanycytes

13 were labeled by injecting the Tat-Cre fusion protein in the third ventricle of Ai14 reporter

14 mice. Then, Tomato-positive tanycytes and Tomato-negative other cells were sorted. RNA

15 obtained from FACS-sorted cells was reverse transcribed using the High-Capacity cDNA

16 Reverse Transcription Kit (4374966, Life Technologies) and a linear pre-amplification step

17 was performed using TaqMan PreAmp Master Mix (4488593, Life Technologies). Real-time

18 PCR was carried out on Applied Biosystems 7900 HT Fast Real-Time PCR System using the

19 following exon-boundary-specific TaqMan Gene Expression Assays (Applied Biosystems):

20 *Il1r1*, Mm00434237_m1; *Il1b*, Mm00434228_m1; *Ikbkg*, Mm00494927_m1; *Nfkb1*,

21 Mm00476361_m1; *Ptgs2*, Mm00478374_m1; *Vcam1*, Mm01320970_m1; *Vimentin*,

22 Mm01333430_m1; *Darpp32* (*Ppp1r1b*), Mm00454892_m1; *Gpr50*, Mm00439147_m1; *Gfap*,

23 Mm01253033_m1; *Npy*, Mm03048253_m1; *Pomc*, Mm00435874_m1; *r18S*,

24 Mm03928990_g1; *Actb*, Mm00607939. Gene expression data were analyzed using SDS

25 2.4.1 and DataAssist 3.0.1 software (Applied Biosystem).

1 **2.10. Western blotting**

2 Primary tanycytes were lysed with 1% cell lysis buffer (Cell Signaling) supplemented with

3 phenylmethylsulfonyl fluorid (PMSF, 0.5 M Sigma-Aldrich). Protein concentrations in the

4 lysates were measured with the Lowry assay. After SDS-PAGE proteins were transferred to

5 nitrocellulose membranes that were incubated with primary antibodies against COX-2 (1:250,

6 sc-1747, Santa Cruz) and GAPDH (1:2,500, ab9485, Abcam) at 4°C overnight followed by

7 incubation with secondary antibodies (1:2,500 HRP-labeled anti-goat IgG, DakoCytomation,

8 Denmark; 1:5,000 HRP-labeled anti-rabbit IgG, Santa Cruz) at room temperature for 1 h.

9 Detection was achieved by chemiluminescence (SuperSignal West Femto Substrate,

10 Thermo Scientific) and a digital detection system (Fusion Solo S, VWR International).

11 **2.11. Immunohistochemistry**

12 To visualize NF-κB activation, serial coronal cryosections (25-μm thick) of NF-κB reporter

13 mice (κ-EGFP) in the area of the ME (bregma −1.35 to −2.46 mm) were processed for

14 immunohistochemistry. First, PFA-fixed sections were washed twice with Tris buffered saline

15 (TBS; Tris 50 mM; NaCl, 150 mM; pH 7.6) for 5 min at room temperature, incubated in TBS

16 containing 0.3% Triton-X100 (TBST, Promega) for 15 min for permeabilisation, and then in

17 TBST containing 5% BSA (Sigma-Aldrich) for 30 min at room temperature. Subsequently,

18 samples were incubated overnight at 4°C with primary antibodies: anti-GFP, 1:500 (ab13970,

19 Abcam); anti-vimentin, 1:500 (5741, New England Biolabs); anti-GFAP, 1:500 (Z033429-2,

20 Dako); anti-Iba1, 1:500 (019-19741, Wako); and anti-collagen-IV 1:1,000, (Abcam #ab6586).

21 Finally, sections were incubated with secondary antibodies: Alexa 488-labeled goat anti-

22 chicken, 1:5,000 (Abcam); CyTM3-conjugated donkey anti-rabbit, 1:1,000

23 (Jackson/Dianova), and Dapi (1 μg/ml, Sigma-Aldrich) for 1 h at room temperature.

24 Frozen cryosections of *Nemo*^FL^ and *Nemo*^glialKO^ mice were fixed in methanol for 10 min at -

25 20°C, washed three times with PBS and incubated in PBS containing 1% BSA for 45 min at

26 room temperature. Subsequently, primary antibodies were added: anti-VCAM1, 1:1,000

27 (550547, BD-Pharmingen) overnight at 4°C. Then, sections were washed with PBS three

28 times before incubation with secondary antibodies: Alexa 488-labled anti-rat IgG, 1:1,000 (A-

11

1   21208, Invitrogen) for 45 min at room temperature. Finally, sections were covered using

2   Mowiol and a coverslip. Pictures were taken with the confocal microscope SP5 (Leica) and

3   10x or 20x objectives. For quantification of VCAM1, the mean grey value of an area of 458

4   mm$^2$ was determined with ImageJ software (National Institutes of Health). All sections were

5   stained in parallel and measured with the same settings.

6   For detecting the reporter tdTomato in *Il1r1*$^{GR/GR}$ mice, 30-µm free-floating sections were

7   incubated overnight in rabbit anti-RFP, 1:1,000 (Abcam) in PBS containing 2% normal

8   donkey serum and 0.3% Triton X-100. Then, sections were incubated for 2 h at room

9   temperature in secondary antibodies: Alexa 555-labeled donkey anti-rabbit IgG, 1:1,000 (Life

10  Technologies).

11  To analyze the specificity of the AAV-based targeting of tanycytes, Ai14 mice were perfused

12  with 4% PFA two weeks after injecting AAV-Dio2-Cre-2A-EGFP (5x10$^{10}$ genomic particles)

13  into the lateral ventricle. To investigate recombination specificity in *GlastCreER*$^{T2}$ mice, we

14  treated *GlastCreER*$^{T2}$::Ai14 mice with tamoxifen. Brains were postfixed in 4% PFA at 4°C

15  overnight. For staining free-floating sections (50 µm) were washed twice in TBS,

16  permeabilized in TBST for 30 min, and incubated in TBST containing 5% BSA for 2 h. Then,

17  sections were incubated in primary antibodies: anti-GFAP, 1:500, (Z033429-2, Dako); anti-

18  CD11b, 1:500 (557397, BD Pharmingen); anti-ppTRH, 1:2,000 (a gift of Martin Wessendorf);

19  and NeuN, 1:500, (MAB377, Millipore) overnight and in Alexa 488-labeled anti-rabbit IgG

20  (1:500, Invitrogen #A-21206) or anti-mouse IgG (1:400, A-31619, Invitrogen) for 2 h. They

21  were mounted as described above.

22  For COX-2 staining, mice were perfused with a solution containing 2% PFA and 0.2%

23  glutaraldehyde. For antigen retrieval, vibratome sections (50-µm thick) of the MBH were

24  incubated in sodium citrate buffer (10 mM, pH 6, 85°C) for 30 min followed by H$_2$O$_2$ treatment

25  (1%, 30 min). After blocking with BSA (5% in PBS + 0.3% Triton-X100) for 2 h, samples were

26  incubated overnight at 4°C with anti-COX-2 (M17-R, Santa Cruz, 1:1,000). Then, biotinylated

27  secondary antibodies against rabbit IgG (1:250, Vector, BR1000) were added for 2 h. For

1  detection we used DAB amplification (A/B Kit, Vector; DAB-Kit, Vector). All sections were

2  stained in parallel and incubated for 1.5 min in the DAB + nickel solution.

### 2.12. *In situ* hybridization for *Nemo* mRNA

4  The *in situ* hybridization for *Nemo* mRNA was performed with the RNAscope® Multiplex

5  Fluorescent Reagent Kit v2 (Advanced Cell Diagnostics, ACD, Hayward, CA, USA). We used

6  a set of 20 double Z probes targeting the first 6 exons of *Nemo* (nucleotides 246-1135 in

7  NM_001136067) which include exon 2 that is floxed in *Nemo*$^{FL}$ animals [25]. Briefly, 20-μm

8  mouse brain cryosections were post-fixed at room temperature in freshly prepared 4% PFA

9  for 15 min, dehydrated with ethanol, backed for 30 min at 37°C, and treated with hydrogen

10  peroxide and protease IV. Then, the sections were incubated with double Z probes for 2 h at

11  40°C, and hybridized sequentially by preamplifiers, amplifiers, HRP-labeled oligonucleotides,

12  followed by TSA® Plus Cyanine 3 probe. Nuclei were counterstained with Dapi. We mounted

13  sections with fluoromount (ACD). After *in situ* hybridization, the sections were imaged with

14  the confocal microscope Leica TCS SP5. Scoring of the *Nemo* mRNA signal in the tanycyte

15  layer of the 3$^{rd}$ ventricle was performed according to the manufacturer's scoring guideline

16  (ACD). The *Nemo* mRNA signal scoring was done as follows: score 1 if 1-3 dots/cell, score 2

17  in 4-9 dots/cell [33]. In at least 4 sections per animal the *Nemo*$^{+}$ cells were counted in the

18  tanycytic layer.  A blinding strategy was followed while scoring the RNAscope images.

### 2.13. Statistical analysis

20  All data are presented as means ± standard error of the mean (SEM). For statistical

21  comparison of two groups we used the Mann Whitney test, unless the sample size per group

22  was bigger than 9 and values were normally distributed. In this case, t-test was applied. For

23  more than two groups the analysis was performed by one-way ANOVA with subsequent

24  Bonferroni post-hoc test or Friedman test. Time-dependent data were analyzed with two-way

25  repeated measures ANOVA followed by Bonferroni post-hoc test. A p value < 0.05 was

26  considered statistically significant. G-Power (Version 3.1.8) was used to analyze power and

27  group size for the experiments.

## 1 3. Results

### 2 3.1. IL-1β directly stimulates NF-κB activity in tanycytes *in vivo*

3 To determine in which cells of the MBH systemic IL-1β induces NF-κB activity, we injected

4 IL-1β (20 μg/kg, i.v.) into NF-κB-EGFP reporter (κ-EGFP) mice, expressing the enhanced

5 green fluorescent protein (EGFP) under the control of an artificial NF-κB promoter [27]. After

6 IL-1β administration, EGFP expression was pronounced in vimentin-positive tanycytes

7 projecting mainly in the VMH (α1-tanycytes) and few tanycytes projecting into the

8 ventromedial ARC (vmARC, dorsal β1-tanycytes, Figure 1, A and B) but not in tanycytes

9 projecting to the capillary bed of the median eminence (ME, ventral β1- and β2-tanycytes

10 Figure 1, A and C) or the dorsomedial ARC (α2-tanycytes). Counting of EGFP$^+$ tanycytes

11 revealed a significant increase after IL-1β injection in comparison to the PBS treated control

12 group (Figure 1D). Additional EGFP expression was detectable in Iba1-positive microglia and

13 blood vessels. Only few GFAP-positive astrocytes in the ME were positive for EGFP

14 (Supplementary Figure 1).

15 Since we had observed that systemic IL-1β stimulates NF-κB activity in tanycytes, we

16 wondered whether IL-1β is able to directly act on tanycytes. Using *in situ* hybridization, a

17 previous study reported a low mRNA signal for *Il1r1*, the essential IL-1 receptor, in the

18 tanycytic layer [34]. However, *in situ* hybridization may not be sensitive enough for the

19 detection of all functionally relevant *Il1r1* expression, as less than 10 IL-1R1 molecules per

20 cell are sufficient to mediate an effect of IL-1β [35]. In tanycytes that were sorted from the

21 MBH of mice we detected mRNA of various components of the IL-1 signaling pathway,

22 including *Il1r1,* at similar levels as in non-tanycytic cells (Figure 1 E, Supplementary Figure

23 2). Using *Il1r1* reporter mice (*Il1r1*$^{GR/GR}$) [28], in which the *Il1r1* locus drives expression of the

24 reporter tdTomato, we confirmed *Il1r1* expression by detecting tdTomato-positive cells in the

25 wall of the 3$^{rd}$ ventricle that projected into VMH and DMH, corresponding to the main

26 localization of NF-κB activity in α1-tanycytes after IL-1β stimulation (Figure 1F). These cells

27 had the typical tanycytic cell shape (Figure 1G).

1 IL-1β is known to upregulate COX-2 in endothelial cells of the BBB [36]. To test whether IL-

2 1β also induces COX-2 in tanycytes, we stained sections 8 h after vehicle and IL-1β injection.

3 As reported previously, COX-2 was found in cells of the hippocampus and in endothelial cells

4 of IL-1β-treated animals with a perinuclear distribution [36; 37] corroborating the specificity of

5 the staining. Interestingly, IL-1β treatment led to a weak but distinct staining of cells in the

6 tanycytic layer (Fig. 1, H and I).


7 **3.2. Tanycytes express pro-inflammatory genes after IL-1β stimulation**

8 In line with the notion that tanycytes are sensitive to IL-1β, we also detected *Il1r1* mRNA in

9 cultured primary tanycytes by RT-PCR (Figure 2A). Interestingly, IL-1β (0.25 µg/ml)

10 enhanced its own expression, which is controlled by NF-κB (Figure 2B), as well as the NF-κB

11 target gene vascular cell adhesion molecule 1 (*Vcam1)* (Figure 2C).  In accordance with the

12 *in vivo* findings (Fig. 1, H and I), IL-1β treatment induced the mRNA levels of the immediate

13 early gene *Ptgs2* encoding COX-2 already after 2 h (Figure 2D). At the protein level COX-2

14 was significantly up-regulated with a more prolonged time course (Figure 2, E and F).

15 To test whether IL-1β enhances COX-2 levels through NF-κB-dependent signaling, primary

16 tanycytes were treated with the IKK specific inhibitor BMS-345541 [38, 25 µM] 30 min before

17 adding IL-1β (0.25 µg/ml). BMS-345541 almost completely suppressed COX-2 induction by

18 IL-1β in primary tanycytes (Figure 2, G and H) confirming that NF-κB signaling mediates the

19 effect of IL-1β. Tanycytes are able to release prostaglandins, such as $PGE_2$ [31; 39-41]. To

20 address the functional relevance of COX-2 in tanycytes, we measured $PGE_2$ in the

21 supernatant. IL-1β stimulated $PGE_2$ release and BMS-345541 blocked the stimulation by IL-

22 1β (Figure 2I). In summary, the data demonstrate that tanycytes respond to IL-1β stimulation

23 by activating NF-κB signaling, up-regulating *Ptgs2* as well as other target genes, and

24 releasing prostanoids which can cause direct effects in the hypothalamus.

### 3.3. Glial *Nemo* knockout reduces NF-κB target genes in α-tanycytes

After having observed that IL-1β activates NF-κB in tanycytes, we aimed to interrupt NF-κB signaling in a cell-specific manner. IL-1β stimulates NF-κB through the canonical signaling pathway that crucially depends on NEMO [42]. To delete *Nemo* we crossed *Nemo*<sup>FL</sup> mice [25] and the *GlastCreER*<sup>T2</sup> line that allows for selective gene deletion in astrocytes and tanycytes but not in microglia or neurons (Supplementary Fig. 3)[26; 29; 43], resulting in *Nemo*<sup>gliaKO</sup> mice. First, we investigated the expression of the validated NF-κB target gene VCAM1 by immunohistochemistry (Figure 3, A-J). Previous studies showed that VCAM1 is up-regulated in the blood-brain barrier and choroid plexus during inflammation and is involved in transmitting inflammatory signals across brain barriers [44-46]. Injecting IL-1β (20 µg/kg, i.v.) to κ-EGFP mice increased VCAM1 staining in vimentin-positive α-tanycytes in which also NF-κB was activated (Supplementary Figure 4). Upon IL-1β treatment, VCAM1 levels were lower in *Nemo*<sup>gliaKO</sup> than in *Nemo*<sup>FL</sup> mice (Figure 3, A-J), in accordance with the notion that the *Nemo* deletion interfered with NF-κB signaling in tanycytes. In addition, we isolated the responsive α-tanycytes, β2-tanycytes and cells in the ARC by laser capture microdissection (LCM, Figure 3K) to quantify mRNA expression of *Nemo* and NF-κB target genes by RT-PCR. In *Nemo*<sup>gliaKO</sup> mice, *Nemo* was deleted in tanycytes, confirming the efficiency of the genetic intervention (Figure 3L). After IL-1β injection, α-tanycytes expressed lower levels of *Ptgs2* mRNA in *Nemo*<sup>gliaKO</sup> mice than in *Nemo*<sup>FL</sup> controls (Figure 3M), while in ARC samples the *Ptgs2* mRNA expression did not significantly differ between the genotypes (Figure 3N). Another NF-κB target gene is the anorexigenic *Pomc* that is expressed in rat tanycytes [47]. In parallel to the *Ptgs2* mRNA expression, we observed a trend towards lower mRNA level of *Pomc* in tanycytes of *Nemo*<sup>gliaKO</sup> mice after IL-1β-treatment in comparison to *Nemo*<sup>FL</sup> controls (Figure 3O). Hence, the glia and tanycyte specific deletion of *Nemo* interfered with the induction of NF-κB target genes *Vcam1*, *Ptgs2*, and possibly *Pomc* that may serve tanycytes to conduct inflammatory signals into the ARC and other hypothalamic centers.

1   To address the possibility that *Nemo*<sup>FL</sup> and *Nemo*<sup>gliaKO</sup> mice could differ in the systemic

2   inflammatory response to IL-1β, we measured cytokine plasma concentrations of IL-1β, IL-6

3   and TNF after IL-1β administration. TNF plasma concentrations did not rise above the

4   detection limit of 20 pg/ml (data not shown). IL-1β and IL-6 plasma concentrations were

5   elevated 4 h after IL-1β injection and decreased over time, independently of the genotype

6   (Figure 3, P and Q). These findings suggest that IL-1β administration leads to a similar

7   inflammatory stimulus in the peripheral compartment of *Nemo*<sup>FL</sup> and *Nemo*<sup>gliaKO</sup> mice.


8   **3.4. IL-1β-induced anorexia depends on glial NEMO**

9   To determine whether deletion of *Nemo* in glial cells leads to a metabolic phenotype under

10  basal conditions we evaluated the body weight under tamoxifen treatment, and  body weight,

11  feeding efficiency, food and water intake, as well as EE and RER using indirect calorimetry, 3

12  weeks after induction of the knockout (Supplementary Figure 5, A-G). These parameters did

13  not differ between *Nemo*<sup>gliaKO</sup> and *Nemo*<sup>FL</sup> control mice. To investigate whether glial NEMO

14  mediates the metabolic effects of IL-1β, we intravenously administered first PBS and after

15  two days IL-1β (20 µg/kg) to the same animals 1 h before their active phase. In accordance

16  with the literature, IL-1β induced anorexia in *Nemo*<sup>FL</sup> mice but this effect was blunted in

17  *Nemo*<sup>gliaKO</sup> littermates with inhibited NF-κB signaling in astrocytes and tanycytes (Figure 4A).

18  During the first 9 h after IL-1β administration, *Nemo*<sup>FL</sup> mice were severely anorexic and

19  consumed less than 0.5 g food, whereas food ingestion was more than doubled in *Nemo*<sup>gliaKO</sup>

20  mice (Figure 4B). At later time points during the inactive phase, food intake did not differ

21  between the groups (data not shown). Therefore, we also analyzed the other metabolic

22  parameters in the active phase within the first 9 h after IL-1β treatment. In parallel to food

23  intake, water consumption was diminished by IL-1β in comparison to PBS treatment (Figure

24  4C). *Nemo*<sup>gliaKO</sup> mice only showed a trend towards more water intake than *Nemo*<sup>FL</sup>

25  littermates. Changes in food intake were reflected by the RER. As the ratio between the

26  amount of $CO_2$ produced and $O_2$ consumed in metabolism, the RER is close to 1 when

27  carbohydrates serve as energy source during feeding but it drops to about 0.7 during fasting

1  when fat metabolism meets the energy demand [48]. IL-1β reduced the RER in *Nemo*<sup>FL</sup>

2  controls in parallel to the lower food intake (Figure 4D). In contrast, glial NF-κB inhibition in

3  *Nemo*<sup>gliaKO</sup> mice led to an almost normal RER confirming that anorexia was ameliorated

4  (Figure 4D). In addition, IL-1β treatment diminished EE in *Nemo*<sup>FL</sup> mice but not in Nemo<sup>gliaKO</sup>

5  animals, although the difference between genotypes missed statistical significance (Figure

6  4E). Due to the lower food intake after IL-1β treatment, *Nemo*<sup>FL</sup> mice showed a loss of body

7  weight 9 h after IL-1β injection which was mitigated in *Nemo*<sup>gliaKO</sup> animals (Figure 4F). As a

8  potential explanation of the increased food intake, *Nemo*<sup>gliaKO</sup> mice had higher mRNA levels

9  of the orexigenic gene *Agrp* in LCM-dissected samples of the ARC than *Nemo*<sup>FL</sup> controls

10  after IL-1β treatment (Figure 4G), while *Pomc* and *Npy* mRNA expression did not differ in the

11  ARC (Figure 4, H and I). These data demonstrate that glial NEMO downregulates *Agrp*

12  expression in the ARC and partially mediates the IL-1β-induced anorexia.

13  **3.5. Fever and lethargy are not affected by glial *Nemo* knockout**

14  To evaluate the role of glial NEMO in fever and lethargy, we determined body temperature

15  and spontaneous home cage locomotion by telemetry. In untreated mice body temperature

16  and locomotion showed a circadian rhythm and did not differ between the *Nemo*<sup>FL</sup> and

17  *Nemo*<sup>gliaKO</sup> genotypes (Supplementary Figure 6, A and B). Also when we subjected the mice

18  to novelty stress, the transient rise in body temperature and locomotion due to the new

19  environment was not affected by the genotype (Supplementary Figure 6, C and D).

20  Injecting IL-1β or PBS led to a transient rise in body temperature in the first h (Figure 4J).

21  However, after 90 min body temperature returned to baseline levels in PBS-treated *Nemo*<sup>FL</sup>

22  mice, while IL-1β significantly increased body temperature in *Nemo*<sup>gliaKO</sup> and *Nemo*<sup>FL</sup> mice

23  (Figure 4J). Importantly, the second IL-1β-induced rise in body temperature was not different

24  in *Nemo*<sup>gliaKO</sup> mice compared with *Nemo*<sup>FL</sup> controls. If anything, the body temperature was

25  higher in *Nemo*<sup>gliaKO</sup> than in *Nemo*<sup>FL</sup> mice 60 – 150 min after IL-1β administration but this

26  difference did not reach statistical significance (Figure 4J). In parallel, the cumulative activity

27  during the first 9 h after injection decreased in response to IL-1β and again did not differ

18

1    between *Nemo*<sup>FL</sup> and *Nemo*<sup>gliaKO</sup> mice (Figure 4K). These data show that glial NEMO is

2    required for IL-1β-induced anorexia but not for fever and lethargy.

### 3.6. Tanycytes mediate the IL-1β-induced anorexic effect

4    The experiments in the κ-EGFP reporter mice (Figure 1, A-D) and the NF-κB-dependent

5    expression of VCAM1 (Figure 3, A-J) suggested that systemic IL-1β activates hypothalamic

6    NF-κB selectively in tanycytes. To investigate whether deleting *Nemo* only in tanycytes

7    suffices to protect animals from IL-1β-induced anorexia, we used a technique to target

8    tanycytes that we have recently described [29]. The approach is based on the combination of

9    local i.c.v. administration of AAV1/2 vectors that get trapped in the ventricle wall and

10   transduce only few parenchymal cells and on the tanycyte-specific promoter *Dio2*. Injecting

11   the vector AAV-Dio2-Cre-2A-EGFP into Ai14 reporter mice, in which tdTomato is a reporter

12   of Cre activity, we confirmed the selectivity for tanycytes (Figure 5A). Four weeks after

13   treating *Nemo*<sup>FL</sup> animals with AAV-Dio2-Cre-2A-EGFP (*Nemo*<sup>tanKO</sup>) to induce recombination

14   in tanycytes or with AAV-Dio2-EGFP as control vector (*Nemo*<sup>Con</sup>), we assessed *Nemo*

15   deletion by detecting *Nemo* mRNA on sections with *in situ* hybridization. Although the *in situ*

16   probe partially hybridizes to the transcript derived from the recombined gene (see Methods

17   section), we found a significant downregulation of the tanycytic *Nemo* signal in *Nemo*<sup>tanKO</sup>

18   mice by 33% (Figure 5, B and C). *Nemo*<sup>tanKO</sup> mice showed no difference in body weight, food

19   and water intake, EE as well as RER under basal conditions (Supplementary Figure 7, A-E),

20   similar to *Nemo*<sup>gliaKO</sup> mice (Supplementary Figure 5). Also after receiving PBS, *Nemo*<sup>Con</sup> and

21   *Nemo*<sup>tanKO</sup> mice did not differ in food intake (Figure 5, D and E). The subsequent treatment

22   with IL-1β (20 μg/kg, i.v.) decreased food consumption of *Nemo*<sup>FL</sup> controls as seen before.

23   However, the IL-1β-induced anorexia was mitigated in *Nemo*<sup>tanKO</sup> mice, in which NF-κB

24   signaling was inhibited in tanycytes (Figure 5, D and E). In parallel, water intake was lower

25   after IL-1β treatment but did not differ between the genotypes (Figure 5F). The deletion of

26   *Nemo* in tanycytes ameliorated the RER reduction after IL-1β treatment, in accordance with

27   the higher food intake (Figure 5G). However, IL-1β treatment reduced EE to a similar extent

1  in *Nemo*<sup>Con</sup> and *Nemo*<sup>tanKO</sup> mice (Figure 5H). In these experiments, the body weight loss due

2  to IL-1β was mitigated by the *Nemo* deletion in tanycytes (Figure 5I). Overall, the data

3  indicate that NF-κB signaling in tanycytes mediates the anorexic effect of IL-1β.

## 4. Discussion

Anorexia is an evolutionarily conserved adaptive response to inflammation and seems to promote the defense against pathogens. In chronic inflammation, this mechanism can go awry and cause life-threatening cachexia. So far, the underlying cellular mechanisms were still unclear. Our study now demonstrates a significant involvement of glial cells in the inflammation-induced anorexia mediated by the NF-κB signaling pathway. Astrocytes [49; 50] and, as shown by the present study, tanycytes are responsive to IL-1β. However, after systemic administration IL-1β activated NF-κB only in few astrocytes of the ME (Supplementary Figure 1). More prominent was the activation of NF-κB in tanycytes, microvessels and microglia. Importantly, the tanycyte-specific deletion of *Nemo* was sufficient to interfere with IL-1β-induced anorexia. Therefore, we conclude that NF-κB signaling in tanycytes mediates inflammation-induced anorexia, at least partially. In contrast, NF-κB signaling in astrocytes has been reported to promote obesity [51-53].

Anorexia adds to the growing list of vital physiological functions that are mediated by tanycytes in the MBH [21]. On the one hand, tanycytes control neurosecretion of the hypothalamic releasing hormones GnRH and TRH [29; 54]. On the other hand, they sense peripheral signals, such as leptin, glucose, and IL-1β according to this study, and transmit the message to neuroendocrine and metabolic centers in the hypothalamus [24; 55]. As a common denominator, tanycytes seem to serve as a switchboard between the periphery and the hypothalamus. They are able to carry out this task due to their location at the interface between blood and CSF or brain parenchyma. From there, they send projections to essential nuclei in the MBH. As shown in this study, tanycytes projecting in the VMH and ARC respond to IL-1β and mediate the anorexigenic effect of systemic IL-1β. We suggest that the open blood-brain barrier in the circumventricular areas allows IL-1β to leave the vessel lumen, to act on tanycytes and to stimulate NF-κB signaling. Fenestrated endothelial cells of the ME and the *pars tuberalis* or other cell types may amplify the pro-inflammatory signal [56] or actively transport IL-1β into the CSF [14; 57]. IL-1β may also induce its own synthesis in the

21

1   hypothalamus [58]. In addition to IL-1β, systemically administered LPS activates NF-κB in

2   tanycytes [59] and induces anorexia. As the anorexic effect of peripheral LPS does not

3   depend on IL1R1 [60], LPS likely acts directly on tanycytes to induce a similar cascade of

4   events as IL-1β.

5   The role of tanycytes in transmitting inflammatory signals from the periphery to the

6   hypothalamus seems to be specifically focused on anorexia, because tanycytic NF-κB did

7   not modulate fever and lethargy. In contrast, endothelial NF-κB mediates IL-1β-induced fever

8   and lethargy but not food intake [17]. Thus, independent mechanisms underlie the various

9   facets of the sickness response [17; 60; 61]. These findings also illustrate that anorexia does

10  not simply reflect an unspecific secondary effect of general sickness but rather an

11  independent effect of systemic inflammation.

12  NF-κB signaling in tanycytes emerges as an attractive target to ameliorate cachexia and to

13  reduce mortality in cancer and chronic infections. Since inhibiting NF-κB is an effective

14  treatment strategy to stop tumor progression [62], blockers of NF-κB signaling may provide

15  dual benefit for patients with malignant diseases. Alternative targets for treating cachexia are

16  IL-1 itself or COX-2 as a downstream gene of NF-κB in tanycytes. Clinical trials and

17  experimental studies show that an anti-IL-1 antibody and COX-2 inhibitors improve anorexia

18  in infections, cancer cachexia, and systemic inflammation [12; 13; 63-65]. The early phase of

19  anorexia is mediated by COX-1, while COX-2 seems to maintain anorexia [13]. Interestingly,

20  this time course is also reflected in our results. After IL-1β treatment, both $Nemo^{gliaKO}$ and

21  $Nemo^{tanKO}$ mice started to eat again earlier than control animals, indicating a predominant

22  effect of the tanycytic COX-2 expression in the later phase of anorexia. Supporting the

23  relevance of tanycytes, cell-specific knockouts of COX-2 in endothelia, neurons and myeloid

24  cells failed to inhibit LPS-induced anorexia [19]. The localization of tanycytes in the ventricle

25  wall may explain why prostaglandin levels are elevated in the CSF during inflammation [60;

26  66]. When injected into the ventricle, $PGE_2$ or PGF2α have an anorexic effect [67; 68].

1    However, the specific prostaglandin downstream of COX-2 that mediates anorexia differs

2    between species and even mouse strains [65; 69-71].

3    Parallel to the NF-κB–COX-2–prostaglandin pathway, there are several other potential

4    mechanisms how tanycytes could mediate anorexia. A candidate is the anorexic

5    gliotransmitter ACBP that is expressed in tanycytes, despite the observation that deletion of

6    ACBP in tanycytes does not affect food intake and body weight on a high-fat diet [72]. In

7    accordance with previous work, we detected *Pomc* mRNA in tanycytes [47]. *Pomc* showed a

8    trend towards lower expression in tanycytes of *Nemo*[gliaKO] mice after systemic IL-1β

9    treatment. Regulation of *Pomc* expression by NF-κB in neurons of the ARC seems to be

10   functionally relevant because deletion of the β subunit of IKK in POMC-positive cells reduced

11   inflammation-induced anorexia [73]. After translation, POMC is cleaved to the active and

12   anorectic peptide α-MSH, which was detected in low concentrations in tanycytes of rats [47].

13   An IL-1β-dependent release of α-MSH by tanycytes could mediate the direct anorexic effect

14   of inflammation.

15   Tanycytes are able to modulate the expression of orexigenic and anorexigenic peptides in

16   the hypothalamus and thereby food intake [74]. IL-1β-treated *Nemo*[gliaKO] mice had a higher

17   expression of *Agrp* mRNA in the ARC compared with *Nemo*[FL] mice. AGRP likely enhances

18   food intake after IL-1β administration, since the parallel injection of AGRP into the CSF

19   abolished anorexia induced by IL-1β [75]. If the release of α-MSH by tanycytes contributes to

20   the IL-1β-induced anorexia, upregulation of AGRP could inhibit the α-MSH effects, since

21   AGRP is a direct antagonist of α-MSH [76]. AGRP neurons also project into the bed nucleus

22   of stria terminalis (BNST), which is an important nucleus for feeding behavior [77]. Upon

23   stimulation, AGRP neurons release GABA and, by inhibiting PKC-δ neurons in the oval part

24   of the BNST, increase food intake under IL-1β and LPS treatment [77; 78].

25   The physiological importance of the central response to inflammation suggests that, in

26   addition to the tanycytic pathway, other mechanisms may contribute to anorexia. Such a

27   scenario would explain why the IL-1β-mediated anorexia was only partly rescued by tanycytic

28   NEMO deficiency (Figure 4, Figure 5). The vagus nerve expresses IL-1R1 and can deliver

1  pro-inflammatory signals from the periphery to the brainstem [79-81]. Vagal afferents end in

2  the nucleus of the solitary tract that is connected to the parabrachial nucleus containing an

3  'emergency circuit' that mediates cancer-induced anorexia [82; 83].

## 5. Conclusions

This study has identified a tanycytic cell population, which directly senses peripheral IL-1β. Triggered by systemic inflammation, tanycytes mount an NF-κB response, express COX-2, release prostaglandins and modulate orexigenic and anorexigenic peptides in the hypothalamus. Inhibition of the NF-κB pathway in tanycytes mitigated anorexia *in vivo*. Overall, tanycytes emerge as an important mediator of inflammation-induced anorexia.

1  ## Author contributions

2  M.S. conceived the study; M.B., H.M.F., D.E., V.P. and M.S. designed the experiments; M.B.,

3  H.M.F., K.S., A.B., D.E. performed and analyzed telemetric measurements; M.B., S.G., and

4  V.P. cultured primary tanycytes and performed cell culture experiments; M.B., H.M.F.

5  investigated mice by indirect calorimetry; M.B., H.M.F., K.S., A.B., D.E. performed feeding

6  studies; M.B., H.M.F., S.S., A.Z., V.N., J.W. and A.B. performed immunohistochemistry; R.H.,

7  R.S.U., N.Q., and X.L. provided essential tools and know-how on IL1R1 and NF-κB signaling;

8  M.B., H.M.F., S.S. and M.S. drafted the manuscript; all authors corrected the manuscript.

9  ## Acknowledgements

21  ## Conflict of interest statement

22  The authors declare no Conflict of interest.

23  ## Appendix A. Supplementary Data

24  Supplementary data related to this article can be found at the website.

# References

[1]     Plata-Salaman, C.R., 1996. Anorexia during acute and chronic disease. Nutrition 12(2):69-78.

[2]     Baracos, V.E., Martin, L., Korc, M., Guttridge, D.C., Fearon, K.C.H., 2018. Cancer-associated cachexia. Nat Rev Dis Primers 4:17105.

[3]     Gautron, L., Laye, S., 2009. Neurobiology of inflammation-associated anorexia. Front Neurosci 3:59.

[4]     Morley, J.E., Thomas, D.R., Wilson, M.M., 2006. Cachexia: pathophysiology and clinical relevance. Am J Clin Nutr 83(4):735-743.

[5]     Hotamisligil, G.S., Erbay, E., 2008. Nutrient sensing and inflammation in metabolic diseases. Nat Rev Immunol 8(12):923-934.

[6]     Wang, A., Huen, Sarah C., Luan, Harding H., Yu, S., Zhang, C., Gallezot, J.-D., et al., 2016. Opposing Effects of Fasting Metabolism on Tissue Tolerance in Bacterial and Viral Inflammation. Cell 166(6):1512-1525.e1512.

[7]     Rao, S., Schieber, A.M., O'Connor, C.P., Leblanc, M., Michel, D., Ayres, J.S., 2017. Pathogen-Mediated Inhibition of Anorexia Promotes Host Survival and Transmission. Cell 168(3):503-516 e512.

[8]     Konsman, J.P., Parnet, P., Dantzer, R., 2002. Cytokine-induced sickness behaviour: mechanisms and implications. Trends Neurosci 25(3):154-159.

[9]     Liu, X., Nemeth, D.P., McKim, D.B., Zhu, L., DiSabato, D.J., Berdysz, O., et al., 2019. Cell-Type-Specific Interleukin 1 Receptor 1 Signaling in the Brain Regulates Distinct Neuroimmune Activities. Immunity.

[10]     Ruud, J., Backhed, F., Engblom, D., Blomqvist, A., 2010. Deletion of the gene encoding MyD88 protects from anorexia in a mouse tumor model. Brain Behav Immun 24(4):554-557.

[11]     Ogimoto, K., Harris, M.K., Jr., Wisse, B.E., 2006. MyD88 is a key mediator of anorexia, but not weight loss, induced by lipopolysaccharide and interleukin-1 beta. Endocrinology 147(9):4445-4453.

[12]    Langhans, W., 2007. Signals generating anorexia during acute illness. Proc Nutr Soc 66(3):321-330.

[13]    Swiergiel, A.H., Dunn, A.J., 2002. Distinct roles for cyclooxygenases 1 and 2 in interleukin-1-induced behavioral changes. J Pharmacol Exp Ther 302(3):1031-1036.

[14]    Banks, W.A., Ortiz, L., Plotkin, S.R., Kastin, A.J., 1991. Human interleukin (IL) 1 alpha, murine IL-1 alpha and murine IL-1 beta are transported from blood to brain in the mouse by a shared saturable mechanism. J Pharmacol Exp Ther 259(3):988-996.

[15]    Engström, L., Ruud, J., Eskilsson, A., Larsson, A., Mackerlova, L., Kugelberg, U., et al., 2012. Lipopolysaccharide-Induced Fever Depends on Prostaglandin E2 Production Specifically in Brain Endothelial Cells. Endocrinology.

[16]    Wilhelms, D.B., Kirilov, M., Mirrasekhian, E., Eskilsson, A., Kugelberg, U.Ö., Klar, C., et al., 2014. Deletion of Prostaglandin E2 Synthesizing Enzymes in Brain Endothelial Cells Attenuates Inflammatory Fever. The Journal of Neuroscience 34(35):11684-11690.

[17]    Ridder, D.A., Lang, M.F., Salinin, S., Roderer, J.P., Struss, M., Maser-Gluth, C., et al., 2011. TAK1 in brain endothelial cells mediates fever and lethargy. J Exp Med 208(13):2615-2623.

[18]    Blomqvist, A., Engblom, D., 2018. Neural Mechanisms of Inflammation-Induced Fever. Neuroscientist 24(4):381-399.

[19]    Nilsson, A., Wilhelms, D.B., Mirrasekhian, E., Jaarola, M., Blomqvist, A., Engblom, D., 2017. Inflammation-induced anorexia and fever are elicited by distinct prostaglandin dependent mechanisms, whereas conditioned taste aversion is prostaglandin independent. Brain Behav Immun 61:236-243.

[20]    Fritz, M., Klawonn, A.M., Nilsson, A., Singh, A.K., Zajdel, J., Wilhelms, D.B., et al., 2016. Prostaglandin-dependent modulation of dopaminergic neurotransmission elicits inflammation-induced aversion in mice. J Clin Invest 126(2):695-705.

[21]    Prevot, V., Dehouck, B., Sharif, A., Ciofi, P., Giacobini, P., Clasadonte, J., 2018. The Versatile Tanycyte: A Hypothalamic Integrator of Reproduction and Energy Metabolism. Endocr Rev 39(3):333-368.

1    [22]    Barahona, M.J., Llanos, P., Recabal, A., Escobar-Acuna, K., Elizondo-Vega, R.,

2    Salgado, M., et al., 2018. Glial hypothalamic inhibition of GLUT2 expression alters satiety,

3    impacting eating behavior. Glia 66(3):592-605.

4    [23]    Collden, G., Balland, E., Parkash, J., Caron, E., Langlet, F., Prevot, V., et al., 2015.

5    Neonatal overnutrition causes early alterations in the central response to peripheral ghrelin.

6    Mol Metab 4(1):15-24.

7    [24]    Balland, E., Dam, J., Langlet, F., Caron, E., Steculorum, S., Messina, A., et al., 2014.

8    Hypothalamic tanycytes are an ERK-gated conduit for leptin into the brain. Cell Metab

9    19(2):293-301.

10    [25]    Schmidt-Supprian, M., Bloch, W., Courtois, G., Addicks, K., Israel, A., Rajewsky, K.,

11    et al., 2000. NEMO/IKK gamma-deficient mice model incontinentia pigmenti. Mol Cell

12    5(6):981-992.

13    [26]    Mori, T., Tanaka, K., Buffo, A., Wurst, W., Kühn, R., Götz, M., 2006. Inducible gene

14    deletion in astroglia and radial glia—A valuable tool for functional and lineage analysis. Glia

15    54(1):21-34.

16    [27]    Tomann, P., Paus, R., Millar, S.E., Scheidereit, C., Schmidt-Ullrich, R., 2016. Lhx2 is

17    a direct NF-kappaB target gene that promotes primary hair follicle placode down-growth.

18    Development 143(9):1512-1522.

19    [28]    Liu, X., Yamashita, T., Chen, Q., Belevych, N., McKim, D.B., Tarr, A.J., et al., 2015.

20    Interleukin 1 type 1 receptor restore: a genetic mouse model for studying interleukin 1

21    receptor-mediated effects in specific cell types. J Neurosci 35(7):2860-2870.

22    [29]    Müller-Fielitz, H., Stahr, M., Bernau, M., Richter, M., Abele, S., Krajka, V., et al., 2017.

23    Tanycytes control the hormonal output of the hypothalamic-pituitary-thyroid axis. Nature

24    communications 8(1):484.

25    [30]    Madisen, L., Zwingman, T.A., Sunkin, S.M., Oh, S.W., Zariwala, H.A., Gu, H., et al.,

26    2010. A robust and high-throughput Cre reporting and characterization system for the whole

27    mouse brain. Nat Neurosci 13(1):133-140.

[31]    Prevot, V., Cornea, A., Mungenast, A., Smiley, G., Ojeda, S.R., 2003. Activation of erbB-1 signaling in tanycytes of the median eminence stimulates transforming growth factor beta1 release via prostaglandin E2 production and induces cell plasticity. J Neurosci 23(33):10622-10632.

[32]    Langlet, F., Levin, B.E., Luquet, S., Mazzone, M., Messina, A., Dunn-Meynell, A.A., et al., 2013. Tanycytic VEGF-A boosts blood-hypothalamus barrier plasticity and access of metabolic signals to the arcuate nucleus in response to fasting. Cell Metab 17(4):607-617.

[33]    Giaretta, P.R., Rech, R.R., Guard, B.C., Blake, A.B., Blick, A.K., Steiner, J.M., et al., 2018. Comparison of intestinal expression of the apical sodium-dependent bile acid transporter between dogs with and without chronic inflammatory enteropathy. J Vet Intern Med 32(6):1918-1926.

[34]    Ericsson, A., Liu, C., Hart, R.P., Sawchenko, P.E., 1995. Type 1 interleukin-1 receptor in the rat brain: distribution, regulation, and relationship to sites of IL-1-induced cellular activation. J Comp Neurol 361(4):681-698.

[35]    Dinarello, C.A., 1996. Biologic basis for interleukin-1 in disease. Blood 87(6):2095-2147.

[36]    Engström, L., Ruud, J., Eskilsson, A., Larsson, A., Mackerlova, L., Kugelberg, U., et al., 2012. Lipopolysaccharide-induced fever depends on prostaglandin E2 production specifically in brain endothelial cells. Endocrinology 153(10):4849-4861.

[37]    Jung, H.Y., Yoo, D.Y., Nam, S.M., Kim, J.W., Kim, W., Kwon, H.J., et al., 2019. Postnatal changes in constitutive cyclooxygenase2 expression in the mice hippocampus and its function in synaptic plasticity. Mol Med Rep 19(3):1996-2004.

[38]    Burke, J.R., Pattoli, M.A., Gregor, K.R., Brassil, P.J., MacMaster, J.F., McIntyre, K.W., et al., 2003. BMS-345541 is a highly selective inhibitor of I kappa B kinase that binds at an allosteric site of the enzyme and blocks NF-kappa B-dependent transcription in mice. J Biol Chem 278(3):1450-1456.

1  [39]  Eskilsson, A., Tachikawa, M., Hosoya, K., Blomqvist, A., 2014. Distribution of

2  microsomal prostaglandin E synthase-1 in the mouse brain. J Comp Neurol 522(14):3229-

3  3244.

4  [40]  De Seranno, S., Estrella, C., Loyens, A., Cornea, A., Ojeda, S.R., Beauvillain, J.C., et

5  al., 2004. Vascular endothelial cells promote acute plasticity in ependymoglial cells of the

6  neuroendocrine brain. J Neurosci 24(46):10353-10363.

7  [41]  de Seranno, S., d'Anglemont de Tassigny, X., Estrella, C., Loyens, A., Kasparov, S.,

8  Leroy, D., et al., 2010. Role of estradiol in the dynamic control of tanycyte plasticity mediated

9  by vascular endothelial cells in the median eminence. Endocrinology 151(4):1760-1772.

10  [42]  Yamaoka, S., Courtois, G., Bessia, C., Whiteside, S.T., Weil, R., Agou, F., et al.,

11  1998. Complementation cloning of NEMO, a component of the IkappaB kinase complex

12  essential for NF-kappaB activation. Cell 93(7):1231-1240.

13  [43]  Robins, S.C., Stewart, I., McNay, D.E., Taylor, V., Giachino, C., Goetz, M., et al.,

14  2013. alpha-Tanycytes of the adult hypothalamic third ventricle include distinct populations of

15  FGF-responsive neural progenitors. Nature communications 4:2049.

16  [44]  Engelhardt, B., Conley, F.K., Butcher, E.C., 1994. Cell adhesion molecules on

17  vessels during inflammation in the mouse central nervous system. Journal of

18  Neuroimmunology 51(2):199-208.

19  [45]  Steffen, B.J., Breier, G., Butcher, E.C., Schulz, M., Engelhardt, B., 1996. ICAM-1,

20  VCAM-1, and MAdCAM-1 are expressed on choroid plexus epithelium but not endothelium

21  and mediate binding of lymphocytes in vitro. Am J Pathol 148(6):1819-1838.

22  [46]  Yousef, H., Czupalla, C.J., Lee, D., Chen, M.B., Burke, A.N., Zera, K.A., et al., 2019.

23  Aged blood impairs hippocampal neural precursor activity and activates microglia via brain

24  endothelial cell VCAM1. Nat Med 25(6):988-1000.

25  [47]  Wittmann, G., Farkas, E., Szilvasy-Szabo, A., Gereben, B., Fekete, C., Lechan, R.M.,

26  2017. Variable proopiomelanocortin expression in tanycytes of the adult rat hypothalamus

27  and pituitary stalk. J Comp Neurol 525(3):411-441.

1  [48]  Tschop, M.H., Speakman, J.R., Arch, J.R., Auwerx, J., Bruning, J.C., Chan, L., et al.,

2  2012. A guide to analysis of mouse energy metabolism. Nat Methods 9(1):57-63.

3  [49]  Ito, H., Yamamoto, N., Arima, H., Hirate, H., Morishima, T., Umenishi, F., et al., 2006.

4  Interleukin-1beta induces the expression of aquaporin-4 through a nuclear factor-kappaB

5  pathway in rat astrocytes. J Neurochem 99(1):107-118.

6  [50]  Molina-Holgado, E., Ortiz, S., Molina-Holgado, F., Guaza, C., 2000. Induction of COX-

7  2 and PGE(2) biosynthesis by IL-1beta is mediated by PKC and mitogen-activated protein

8  kinases in murine astrocytes. Br J Pharmacol 131(1):152-159.

9  [51]  Garcia-Caceres, C., Balland, E., Prevot, V., Luquet, S., Woods, S.C., Koch, M., et al.,

10 2019. Role of astrocytes, microglia, and tanycytes in brain control of systemic metabolism.

11 Nat Neurosci 22(1):7-14.

12 [52]  Douglass, J.D., Dorfman, M.D., Fasnacht, R., Shaffer, L.D., Thaler, J.P., 2017.

13 Astrocyte IKKbeta/NF-kappaB signaling is required for diet-induced obesity and

14 hypothalamic inflammation. Mol Metab 6(4):366-373.

15 [53]  Zhang, Y., Reichel, J.M., Han, C., Zuniga-Hertz, J.P., Cai, D., 2017. Astrocytic

16 Process Plasticity and IKKbeta/NF-kappaB in Central Control of Blood Glucose, Blood

17 Pressure, and Body Weight. Cell Metab 25(5):1091-1102 e1094.

18 [54]  Parkash, J., Messina, A., Langlet, F., Cimino, I., Loyens, A., Mazur, D., et al., 2015.

19 Semaphorin7A regulates neuroglial plasticity in the adult hypothalamic median eminence.

20 Nature communications 6:6385.

21 [55]  Benford, H., Bolborea, M., Pollatzek, E., Lossow, K., Hermans-Borgmeyer, I., Liu, B.,

22 et al., 2017. A sweet taste receptor-dependent mechanism of glucosensing in hypothalamic

23 tanycytes. Glia 65(5):773-789.

24 [56]  Knoll, J.G., Krasnow, S.M., Marks, D.L., 2017. Interleukin-1beta signaling in

25 fenestrated capillaries is sufficient to trigger sickness responses in mice. J

26 Neuroinflammation 14(1):219.

1   [57]   Erickson, M.A., Banks, W.A., 2018. Neuroimmune Axes of the Blood-Brain Barriers

2   and Blood-Brain Interfaces: Bases for Physiological Regulation, Disease States, and

3   Pharmacological Interventions. Pharmacol Rev 70(2):278-314.

4   [58]   Skelly, D.T., Hennessy, E., Dansereau, M.A., Cunningham, C., 2013. A systematic

5   analysis of the peripheral and CNS effects of systemic LPS, IL-1beta, [corrected] TNF-alpha

6   and IL-6 challenges in C57BL/6 mice. PLoS ONE 8(7):e69123.

7   [59]   de Vries, E.M., Nagel, S., Haenold, R., Sundaram, S.M., Pfrieger, F.W., Fliers, E., et

8   al., 2016. The Role of Hypothalamic NF-kappaB Signaling in the Response of the HPT-Axis

9   to Acute Inflammation in Female Mice. Endocrinology 157(7):2947-2956.

10   [60]   Matsuwaki, T., Shionoya, K., Ihnatko, R., Eskilsson, A., Kakuta, S., Dufour, S., et al.,

11   2017. Involvement of interleukin-1 type 1 receptors in lipopolysaccharide-induced sickness

12   responses. Brain Behav Immun 66(Supplement C):165-176.

13   [61]   Serrats, J., Schiltz, J.C., García-Bueno, B., van Rooijen, N., Reyes, T.M., Sawchenko,

14   P.E., 2010. Dual Roles for Perivascular Macrophages in Immune-to-Brain Signaling. Neuron

15   65(1):94-106.

16   [62]   Taniguchi, K., Karin, M., 2018. NF-kappaB, inflammation, immunity and cancer:

17   coming of age. Nat Rev Immunol 18(5):309-324.

18   [63]   Prado, B.L., Qian, Y., 2019. Anti-cytokines in the treatment of cancer cachexia. Ann

19   Palliat Med 8(1):67-79.

20   [64]   Maccio, A., Madeddu, C., Gramignano, G., Mulas, C., Floris, C., Sanna, E., et al.,

21   2012. A randomized phase III clinical trial of a combined treatment for cachexia in patients

22   with gynecological cancers: evaluating the impact on metabolic and inflammatory profiles

23   and quality of life. Gynecologic oncology 124(3):417-425.

24   [65]   Nilsson, A., Elander, L., Hallbeck, M., Örtegren Kugelberg, U., Engblom, D.,

25   Blomqvist, A., 2017. The involvement of prostaglandin E2 in interleukin-1β evoked anorexia

26   is strain dependent. Brain, Behavior, and Immunity 60:27-31.

[66]   Eskilsson, A., Matsuwaki, T., Shionoya, K., Mirrasekhian, E., Zajdel, J., Schwaninger, M., et al., 2017. Immune-Induced Fever Is Dependent on Local But Not Generalized Prostaglandin E2 Synthesis in the Brain. J Neurosci 37(19):5035-5044.

[67]   Skibicka, K.P., Alhadeff, A.L., Leichner, T.M., Grill, H.J., 2011. Neural controls of prostaglandin 2 pyrogenic, tachycardic, and anorexic actions are anatomically distributed. Endocrinology 152(6):2400-2408.

[68]   Tachibana, T., Nakai, Y., Makino, R., Khan, M.S.I., Cline, M.A., 2017. Effect of central and peripheral injection of prostaglandin E2 and F2α on feeding and the crop-emptying rate in chicks. Prostaglandins & Other Lipid Mediators 130:30-37.

[69]   Ohinata, K., Suetsugu, K., Fujiwara, Y., Yoshikawa, M., 2006. Activation of prostaglandin E receptor EP4 subtype suppresses food intake in mice. Prostaglandins & Other Lipid Mediators 81(1–2):31-36.

[70]   Pecchi, E., Dallaporta, M., Thirion, S., Salvat, C., Berenbaum, F., Jean, A., et al., 2006. Involvement of central microsomal prostaglandin E synthase-1 in IL-1beta-induced anorexia. Physiol Genomics 25(3):485-492.

[71]   Smith, W.L., Urade, Y., Jakobsson, P.J., 2011. Enzymes of the cyclooxygenase pathways of prostanoid biosynthesis. Chem Rev 111(10):5821-5865.

[72]   Bouyakdan, K., Martin, H., Lienard, F., Budry, L., Taib, B., Rodaros, D., et al., 2019. The gliotransmitter ACBP controls feeding and energy homeostasis via the melanocortin system. J Clin Invest 129(6):2417-2430.

[73]   Jang, P.G., Namkoong, C., Kang, G.M., Hur, M.W., Kim, S.W., Kim, G.H., et al., 2010. NF-kappaB activation in hypothalamic pro-opiomelanocortin neurons is essential in illness- and leptin-induced anorexia. J Biol Chem 285(13):9706-9715.

[74]   Uranga, R.M., Millan, C., Barahona, M.J., Recabal, A., Salgado, M., Martinez, F., et al., 2017. Adenovirus-mediated suppression of hypothalamic glucokinase affects feeding behavior. Sci Rep 7(1):3697.

[75]   DeBoer, M.D., Scarlett, J.M., Levasseur, P.R., Grant, W.F., Marks, D.L., 2009. Administration of IL-1beta to the 4th ventricle causes anorexia that is blocked by agouti-

related peptide and that coincides with activation of tyrosine-hydroxylase neurons in the nucleus of the solitary tract. Peptides 30(2):210-218.

[76]    Ollmann, M.M., Wilson, B.D., Yang, Y.K., Kerns, J.A., Chen, Y., Gantz, I., et al., 1997. Antagonism of central melanocortin receptors in vitro and in vivo by agouti-related protein. Science 278(5335):135-138.

[77]    Betley, J.N., Cao, Z.F., Ritola, K.D., Sternson, S.M., 2013. Parallel, redundant circuit organization for homeostatic control of feeding behavior. Cell 155(6):1337-1350.

[78]    Wang, Y., Kim, J., Schmit, M.B., Cho, T.S., Fang, C., Cai, H., 2019. A bed nucleus of stria terminalis microcircuit regulating inflammation-associated modulation of feeding. Nature communications 10(1):2769.

[79]    Bret-Dibat, J.L., Bluthe, R.M., Kent, S., Kelley, K.W., Dantzer, R., 1995. Lipopolysaccharide and interleukin-1 depress food-motivated behavior in mice by a vagal-mediated mechanism. Brain Behav. Immun. 9(3):242-246.

[80]    Ek, M., Engblom, D., Saha, S., Blomqvist, A., Jakobsson, P.J., Ericsson-Dahlstrand, A., 2001. Inflammatory response: pathway across the blood-brain barrier. Nature 410(6827):430-431.

[81]    Hosoi, T., Okuma, Y., Matsuda, T., Nomura, Y., 2005. Novel pathway for LPS-induced afferent vagus nerve activation: possible role of nodose ganglion. Auton Neurosci 120(1-2):104-107.

[82]    Campos, C.A., Bowen, A.J., Han, S., Wisse, B.E., Palmiter, R.D., Schwartz, M.W., 2017. Cancer-induced anorexia and malaise are mediated by CGRP neurons in the parabrachial nucleus. Nat Neurosci 20(7):934-942.

[83]    Ruud, J., Blomqvist, A., 2007. Identification of rat brainstem neuronal structures activated during cancer-induced anorexia. J Comp Neurol 504(3):275-286.

1 **FIGURE LEGENDS**

2 **Figure 1: Systemic IL-1β activates NF-κB in tanycytes.**
3 (A) Representative immunostainings of the mediobasal hypothalamus (MBH) of κ-EGFP reporter mice
4 8 h after IL-1β (20 µg/kg, i.v.) or PBS injection. EGFP (A, white; B and C, cyan) reflecting NF-κB
5 activity (cell bodies, arrow; projections, arrowheads) of tanycytes (vimentin, magenta). Asterisks
6 indicate EGFP⁺ microglia. Scale bar, 100 µm. (B, C) Higher magnification of boxed area in A (green
7 box, B; yellow box, C). Scale bar, 20 µm. (D) Number of EGFP⁺ tanycytes in the MBH per section.
8 Means ± SEM *p<0.01 (Mann-Whitney test, n=3 sections/mouse of 3 mice/group). (E) mRNA
9 expression of various genes of the IL-1β signaling pathway in FACS-sorted tanycytes (red, tdTomato-
10 positive) and non-tanycytic cells (gray, tdTomato-negative). Medians ± quartiles. (F, G) tdTomato
11 immunostainings (white) in tanycytes of *Il1r1*^GR/GR^ mice indicating *Il1r1* transcription. Staining was
12 performed 6 h after LPS treatment (120 µg/kg, i.p.). Yellow arrowheads indicate contact points of
13 tanycytic endings and blood vessels. Scale bar, 150 µm (F) and 20 µm (G). (H, I) Representative
14 COX-2 immunostainings 8 h after i.v. injection of NaCl (H) or IL-1β (20 µg/kg, I). In the hippocampus
15 positive cells could be identified after NaCl injection. After IL-1β treatment, COX-2-positive cells were
16 detectable in the tanycytic layer and bigger blood vessels (I). Arrowheads, COX-2-positive cell bodies;
17 yellow box, magnified field; scale bar, 100 µm (hypothalamic overview), 50 µm (vessels,
18 hippocampus), 10 µm (magnified field).

19 **Figure 2: IL-1β stimulates the release of PGE₂ from tanycytes by activating the NF-κB pathway.**
20 (A) After treating primary tanycytes with IL-1β (0.25 µg/ml) or PBS for 24 h, *Il1r1* (172 bp) and *Gapdh*
21 (122 bp) mRNA were detected by RT-PCR (representative images of the agarose gels). (B-D)
22 Expression of *Il1b* (B), *Vcam1* (C) and *Ptgs*2 (D) over time after IL-1β stimulation of primary tanycytes.
23 Two-way ANOVA for treatment: *Il1b*, $F_{(1,20)}$=21.33, p=0.0002; *Vcam1*, $F_{(1,20)}$=12.09, p=0.0024; *Ptgs2*,
24 $F_{(1,19)}$=6.11, p=0.023. *p<0.05, **p<0.01, ***p<0.001 (Bonferroni post-test, n=3 independent primary
25 cell cultures of 3 wells/experiment). (E, F) Western blots of COX-2 after IL-1β (0.25 µg/ml) stimulation
26 of primary tanyctes. GAPDH served as a loading control. Quantification of COX-2 protein levels at
27 various time points after IL-1β stimulation (F). Two-way ANOVA for treatment, $F_{(1,20)}$=41.57, p<0.0001.
28 (Bonferroni post test, n=3 independent primary cell cultures of 3 wells/experiment). (G, H)
29 Pretreatment with the IKK inhibitor BMS-345541 (BMS, 25 µM) blocked the induction of COX-2 by IL-
30 1β (0.25 µg/ml) in primary tanycytes. Quantification of COX-2 protein levels (H). Two-way ANOVA;
31 Bonferroni post test, n=2 independent primary cell cultures of 3 wells/experiment. (I) Quantification of
32 PGE₂ levels in the medium showed that IL-1β stimulated PGE₂ secretion in an IKK-dependent
33 manner. For IL-1β treatment: $F_{(1,14)}$= 8.745, p=0.0104; for BMS treatment, $F_{(1,14)}$=15.48, p=0.0015;
34 interaction, $F_{(1,14)}$=14.08, p=0.0021, post-test: *p=0.017 (Two-way ANOVA; Bonferroni post-test, n=3
35 independent primary cell cultures of 3 wells/experiment).

36 **Figure 3: Glial deletion of *Nemo* (*Nemo*^gliaKO^) interferes with the induction of NF-κB target genes**
37 **by IL-1β.**
38 (A-I) Immunohistochemistry showed that IL-1β (20 µg/kg, i.v.) up-regulated the NF-κB target gene
39 VCAM1 in α-tanycytes of *Nemo*^FL^ but not of *Nemo*^gliaKO^ mice. Representative immunostainings of
40 VCAM1 in coronal mediobasal hypothalamus (MBH) sections of *Nemo*^FL^ (A-C) and *Nemo*^gliaKO^ (D-F)
41 mice 8 h after IL-1β treatment and PBS treated *Nemo*^FL^ mice (G-I). (B), (C), (E), (F) and (H), (I) are
42 higher magnifications of the boxed areas in (A), (D) and (G), respectively. Scale bar, 100 µm. (J)
43 Quantification of VCAM1 staining in α-tanycytes projecting mainly into the VMH at various time points
44 after IL-1β administration. Values are means ± SEM. Two-way ANOVA for genotype, $F_{(1, 29)}$=4.46,
45 p=0.044. *p<0.05 (Bonferroni post-test, n=7-8 animals per group). (K) Nissl-stained coronal section of
46 the MBH showing microdissected areas of the tanycytic layer and arcuate nucleus (ARC). ME, median
47 eminence; 3V, 3rd ventricle; scale bar, 100 µm. (L) Representative agarose gels after RT-PCR for
48 *Nemo* and *β-actin* in microdissected tanycytes from *Nemo*^FL^ and *Nemo*^gliaKO^ mice. (M, N) *Ptgs2* mRNA
49 was reduced in tanycytes of *Nemo*^gliaKO^ mice in comparison to *Nemo*^FL^ controls 4 h after IL-1β
50 treatment (M). In contrast, there was no difference in the ARC (N). *p<0.05 (Mann-Whitney test, n=6-8
51 mice/group). (O) *Pomc* mRNA was reduced in tanycytes of *Nemo*^gliaKO^ mice in comparison to *Nemo*^FL^
52 controls 4 h after IL-1β treatment (Mann-Whitney test, n=6-8 mice/group). (P, Q) Plasma
53 concentrations of IL-6 (M) and IL-1β (N) did not differ between *Nemo*^FL^ and *Nemo*^gliaKO^ animals after
54 intravenous IL-1β injection. Values are means ± SEM (n=6-8 mice/group).

1  **Figure 4: Glial deletion of *Nemo* (*Nemo*[gliaKO]) mitigates IL-1β-induced anorexia but has no effect**
2  **on body temperature and locomotor activity.**
3  (A) The IL-1β-induced anorexia was mitigated by glial deletion of *Nemo*. *Nemo*[FL] (blue) and *Nemo*[gliaKO]
4  mice (purple) were treated with PBS and two days later with IL-1β (20 µg/kg, i.v., 1 h before start of
5  the active phase). Cumulative food intake is shown. (B-D) Food ingestion (B), water intake (C), and
6  the respiratory exchange ratio (RER, D) of *Nemo*[FL] and *Nemo*[gliaKO] mice over 9 h after IL-1β or PBS
7  treatment. Means ± SEM. Repeated-measures ANOVA for the interaction between treatment and
8  genotype; $F_{(1,20)}=5.56$, $p=0.029$ (B); $F_{(1,20)}=4.82$, $p=0.04$ (D). *$p<0.05$; **$p<0.01$ (Bonferroni post-test);
9  ns, non-significant. (E) The reduction in energy expenditure by IL-1β (ΔEE) showed a trend towards
10 normalization in *Nemo*[gliaKO] mice in comparison to *Nemo*[FL] controls. Means ± SEM (t-test, n=10-12
11 mice/group). (F) Loss of body weight of *Nemo*[gliaKO] and *Nemo*[FL] mice 9 h after IL-1β administration.
12 **$p<0.01$ (Mann Whitney test, n=5-6 mice/group). (G) *Agrp* mRNA levels in the ARC were higher in
13 *Nemo*[gliaKO] mice than in *Nemo*[FL] controls 4 h after IL-1β injection. **$p<0.01$ (Mann Whitney test, n=6
14 mice/group). (H, I) Expression of *Pomc* mRNA (H) and *Npy* mRNA (I) in ARC were unchanged in
15 *Nemo*[gliaKO] mice compared with *Nemo*[FL] controls 4 h after IL-1β injection (Mann-Whitney test, n=6
16 mice/group). (J) After a lag time of about 60 min, IL-1β (i.v., 20 µg/kg) increased the body temperature
17 of *Nemo*[FL] and *Nemo*[gliaKO] mice in comparison to PBS-treated conditions. There was a trend towards
18 higher body temperatures in *Nemo*[gliaKO] than in *Nemo*[FL] mice after IL-1β treatment. Repeated-
19 measures ANOVA for genotype, $F_{(1,2304)}=4.35$, $p=0.052$. ns, non-significant (Bonferroni post-test). (K)
20 In parallel, IL-1β treatment but not genotype reduced locomotor activity. One-way ANOVA, $F_{(2,38)}=6.56$,
21 $p=0.0037$. *$p<0.05$, **$p<0.01$, ns, non-significant (Bonferroni post-test, n=9-19 mice/group).

22 **Figure 5: Tanycytic deletion of *Nemo* increases food intake after IL-1β treatment.**
23 (A) Injecting AAV-Dio2-Cre-2A-EGFP into the ventricle of Ai14 mice led to selective expression of the
24 Cre reporter tdTomato (weight / red) in tanycytes. Blue, Dapi; scale bar, 100 µm. (B) *Nemo* mRNA
25 (red) in the tanycyte layer. Representative *in situ* hybridization is shown. Tanycyte-specific *Nemo*
26 knockout mice (*Nemo*[tanKO]) were generated by injecting AAV-Dio2-Cre-2A-EGFP in the lateral ventricle
27 of *Nemo*[FL] mice. *Nemo*[FL] mice that received control AAV-Dio2-EGFP are called *Nemo*[con]. Gray, Dapi;
28 scale bar, 1 µm. (C) Numbers of *Nemo*-positive cells in tanycytic layer as determined by *in situ*
29 hybridization. *$p<0.05$ (t-test). Values are means ± SEM. (D) IL-1β-induced anorexia was alleviated in
30 *Nemo*[tanKO] mice in comparison to *Nemo*[FL] controls. Four weeks after virus injection, mice were treated
31 with PBS and two days later with IL-1β (20 µg/kg). Cumulative food intake at various time points after
32 IL-1β treatment is shown. Values are means ± SEM (n=7-11 mice/group). (E-G) Food ingestion (E),
33 water intake (F), and the respiratory exchange ratio (RER, G) of *Nemo*[con] and *Nemo*[tanKO] mice during a
34 period of 6 h after IL-1β or PBS treatment are depicted. Means ± SEM and individual values are
35 shown. Repeated-measures ANOVA for interaction of treatment and genotype; $F_{(1,15)}=4.26$, $p=0.057$
36 (E); $F_{(1,15)}=7.69$, $p=0.014$ (G). *$p<0.05$ (Bonferroni post-test). (H) The reduction in energy expenditure
37 by IL-1β (ΔEE) was similar in *Nemo*[tanKO] mice and in *Nemo*[con] controls. Values are means ± SEM (t-
38 test, n=8-10 mice/group). (I) Body weight loss 6 h after IL-1β administration was reduced in *Nemo*[tanKO]
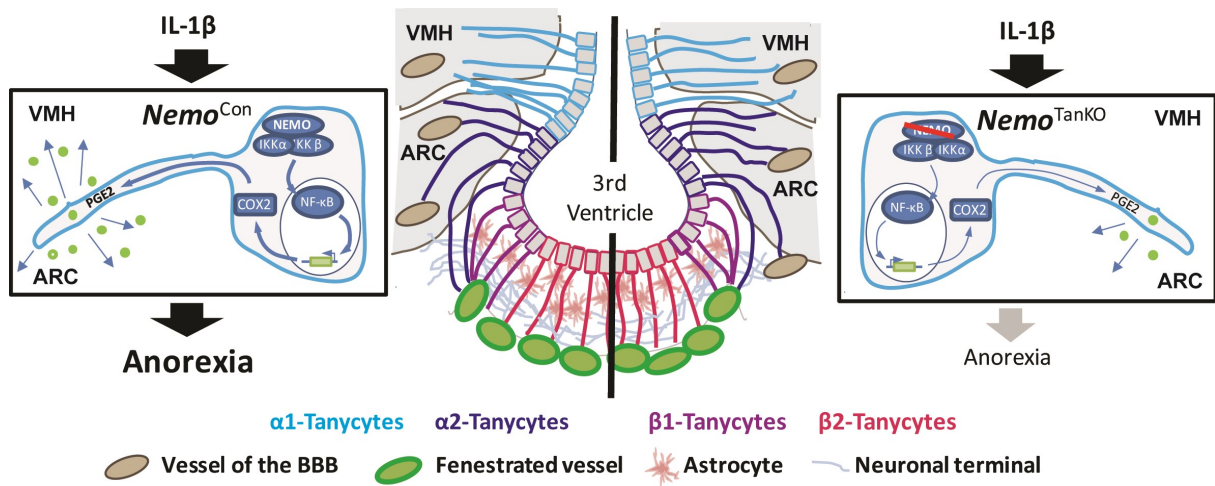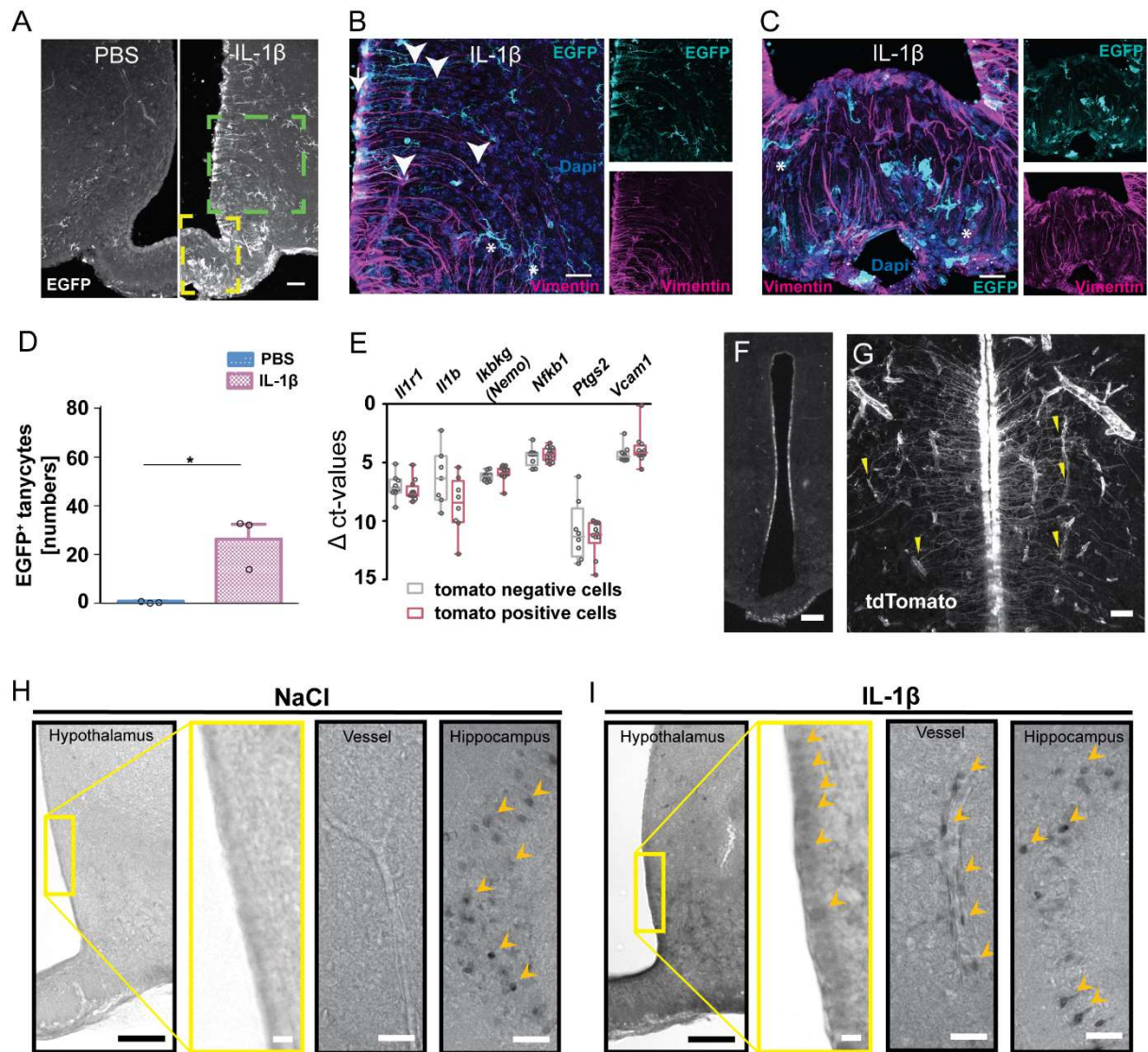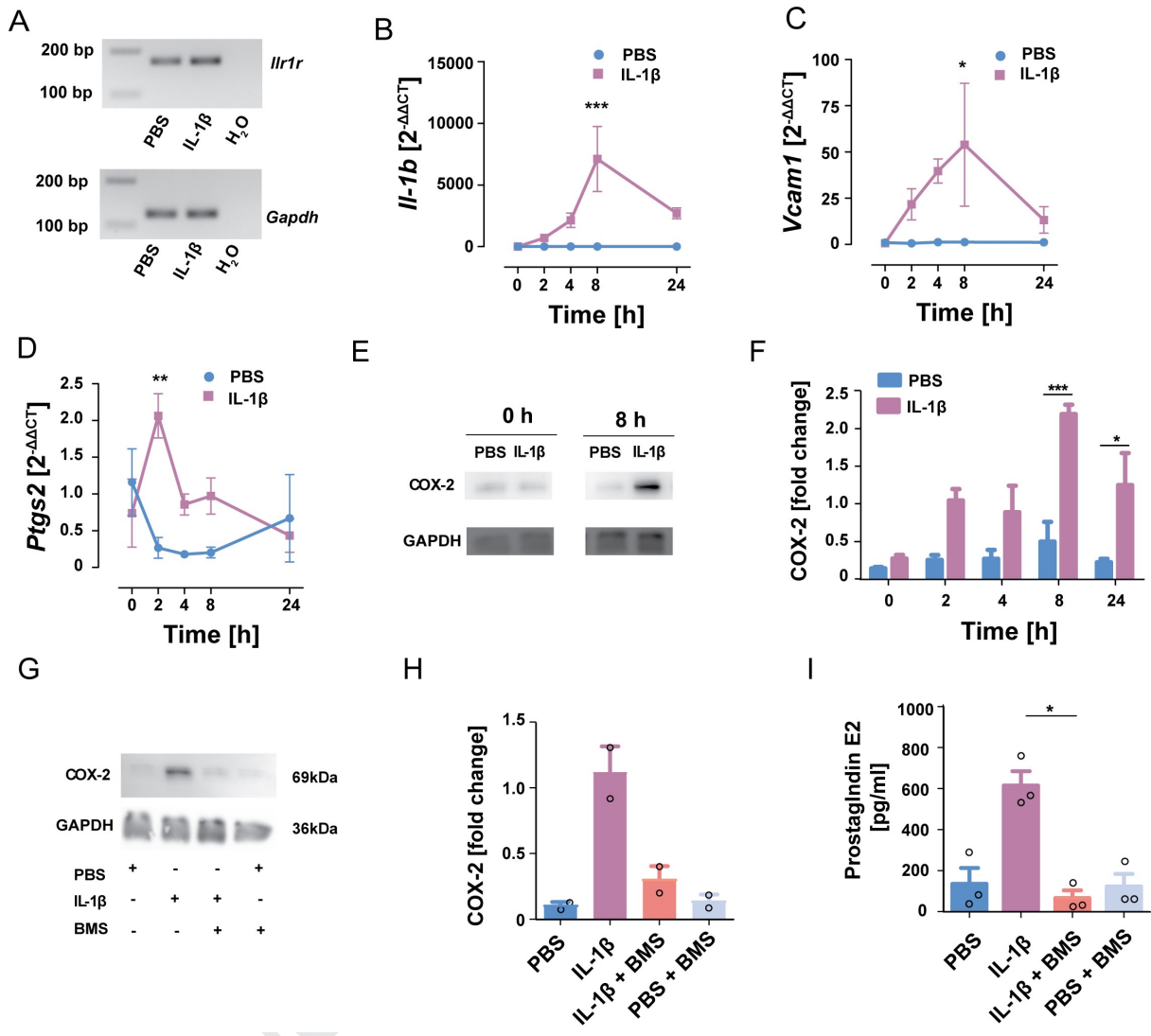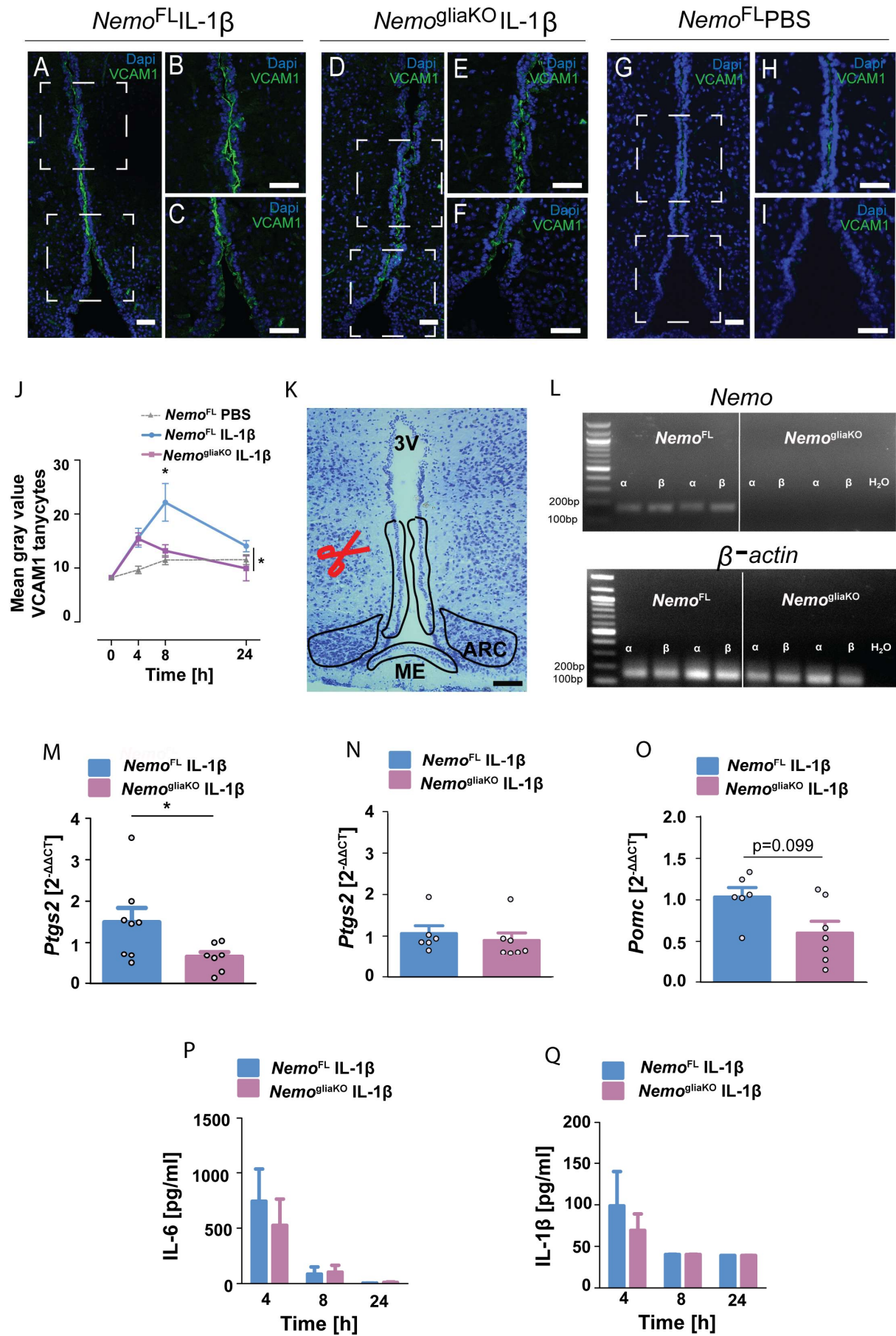39 mice. *$p<0.05$ (Mann-Whitney test, n=8-9 mice/group).

Graphical abstract

Figure 1

Figure 2

Figure 3



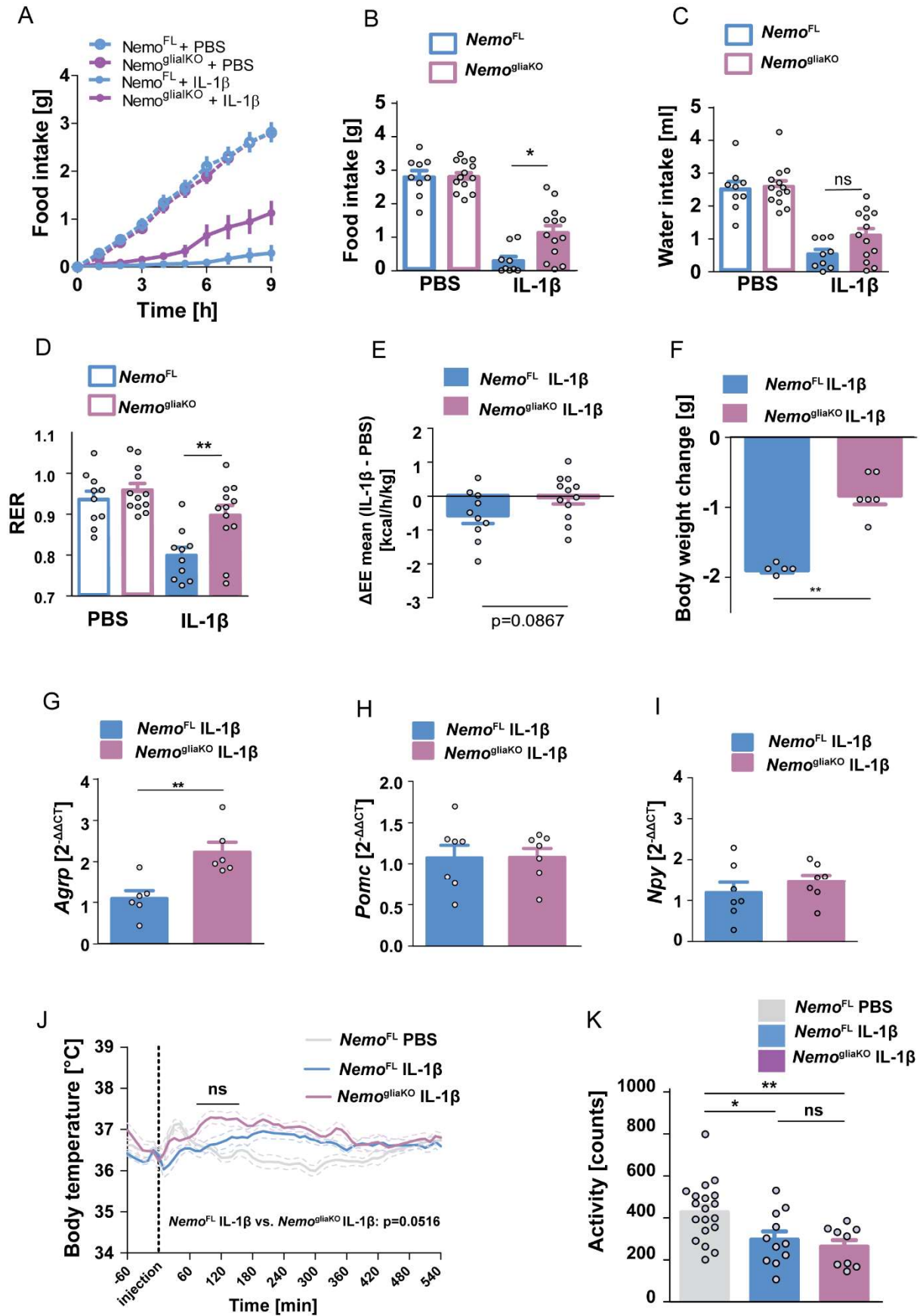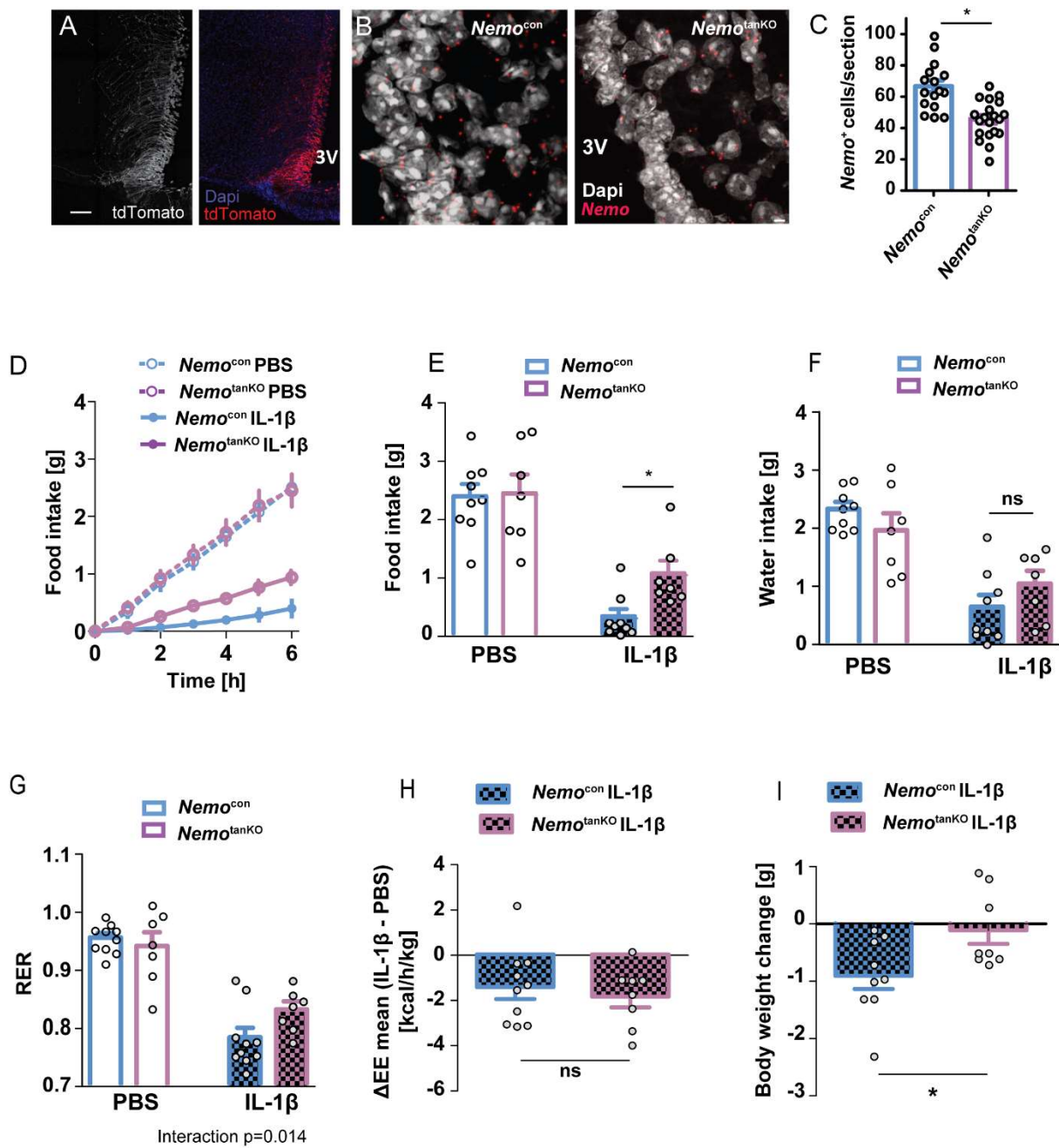$Nemo^{FL}$IL-1β   $Nemo^{gliaKO}$IL-1β   $Nemo^{FL}$PBS

Figure 4

Figure 5

## Highlights

- Systemic IL-1β activates NF-κB in tanycytes.

- IL-1β induces the expression of *Ptgs2* (*Cox-2)* and the release of $PGE_2$ from tanycytes.

- NEMO-dependent NF-κB signaling in tanycytes is required for the anorexia induced by IL-1β.

- Tanycytes are not involved in fever and lethargy induced by IL-1β.

**Declaration of interests**

☒ The authors declare that they have no known competing financial interests or personal relationships that could have appeared to influence the work reported in this paper.

☐The authors declare the following financial interests/personal relationships which may be considered as potential competing interests: